

## Accepted Manuscript

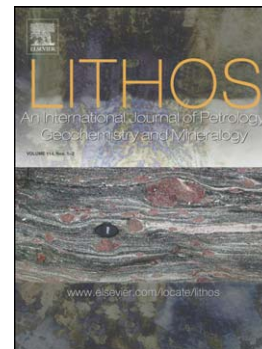
Collision vs. subduction-related magmatism: two contrasting ways of granite formation and implications for crustal growth

J.-F. Moyen, O. Laurent, C. Chelle-Michou, S. Couzinié, O. Vanderhaeghe, A. Zeh, A. Villaros, V. Gardien

PII: S0024-4937(16)30306-1  
DOI: doi:[10.1016/j.lithos.2016.09.018](https://doi.org/10.1016/j.lithos.2016.09.018)  
Reference: LITHOS 4079

To appear in: *LITHOS*

Received date: 4 February 2016  
Revised date: 2 September 2016  
Accepted date: 10 September 2016



Please cite this article as: Moyen, J.-F., Laurent, O., Chelle-Michou, C., Couzinié, S., Vanderhaeghe, O., Zeh, A., Villaros, A., Gardien, V., Collision vs. subduction-related magmatism: two contrasting ways of granite formation and implications for crustal growth, *LITHOS* (2016), doi:[10.1016/j.lithos.2016.09.018](https://doi.org/10.1016/j.lithos.2016.09.018)

This is a PDF file of an unedited manuscript that has been accepted for publication. As a service to our customers we are providing this early version of the manuscript. The manuscript will undergo copyediting, typesetting, and review of the resulting proof before it is published in its final form. Please note that during the production process errors may be discovered which could affect the content, and all legal disclaimers that apply to the journal pertain.

# Collision vs. subduction-related magmatism: two contrasting ways of granite formation and implications for crustal growth

Moyen, J.-F.<sup>1,+</sup>, Laurent, O.<sup>2,3</sup>, Chelle-Michou, C.<sup>1,4</sup>, Couzinié, S.<sup>1</sup>, Vanderhaeghe, O.<sup>5</sup>, Zeh, A.<sup>2,6</sup>, Villaros, A.<sup>7</sup> & Gardien, V.<sup>8</sup>

1. Université de Lyon, Laboratoire Magmas et Volcans, UJM-UBP-CNRS-IRD, 23 rue Dr. Paul Michelon, 42023 Saint Etienne, France.
2. J.W. Goethe Universität, Institut für Geowissenschaften, Altenhöferallee 1, D-60438 Frankfurt am Main, Germany
3. Université de Liège, Département de Géologie B20, Quartier Agora, allée du six Août 12, B-4000 Liège, Belgium
4. Université de Genève, Département des Sciences de la Terre, rue des Maraichers, 13, 1205 Genève, Switzerland
5. GET, UMR 5563 CNRS / UR 234 IRD / UPS, 14, avenue Édouard Belin, 31400 Toulouse, France
6. Now at Karlsruhe Institute für Technologie (KIT), Institute of Applied Geosciences, Adenauerring 20b, building 50.40, 76131 Karlsruhe, Germany
7. Univ d'Orléans, ISTO, UMR 7327, 45071, Orléans, France.
8. Université de Lyon, Université Lyon 1, ENS de Lyon, CNRS, UMR 5276 LGL-TPE, F-69622, Villeurbanne, France

+ Corresponding author. jean.francois.moyen@univ-st-etienne.fr

## 1 Introduction

The continental crust has been extracted from the mantle throughout Earth history,. In contrast with the mafic oceanic crust, the continental crust is largely made up of low-density, buoyant quartzofeldspathic material, in particular granitoid rocks, which enable its long-term stability and preservation at the surface of our planet (Rudnick and Gao, 2003; Hawkesworth et al., 2010; Dhuime et al., 2011). However, granitoid rocks cannot be directly derived from mantle melting (Rudnick, 1995): as such, felsic melts are not in equilibrium with an ultramafic mantle assemblage. Hence, two main mechanisms allow the formation of granitoid magmas: (i) differentiation, through crystallization or melting, of mantle-derived basaltic material; or (ii) partial melting of felsic, meta-igneous or meta-sedimentary rocks, either containing free water or hydrous minerals making them prone to melting. Whereas the first mechanism allows the formation of new continental crust, since it is ultimately a high-degree fractionation process of mantle material, the second mechanism reworks pre-existing continental rocks and therefore does not represent any addition to the crustal volume. Thus,

unravelling the respective contribution of these two different mechanisms in the genesis of granitoid suites is necessary to understand the mechanisms of continental crust growth and differentiation through time.

In the modern Earth, granites are primarily formed along convergent plate boundaries (Barbarin, 1999). During lithospheric convergence, the lithospheric mantle is (mostly) recycled through foundering in deeper mantle domains, whereas the crust (either continental, or oceanic) can have two distinct fates: (1) subduction along with the lithospheric mantle and recycling; or (2) accretion against the overriding plate followed by a potential reworking (Vanderhaeghe 2012). Each segment of a convergent plate boundary has its own balance between the two processes, depending on the degree of coupling (allowing recycling) or decoupling (promoting tectonic accretion) between the lower plate crust and its underlying lithospheric mantle. This results in a range of situations with extreme end-members corresponding to the classical “subduction” (pure recycling of the crust of the lower plate), and “continental collision” (pure tectonic accretion of the lower plate crust). In fact, the two different mechanisms of granite formation described above can be correlated at the first order to these two distinct geodynamic scenarios. Above subduction zones, fluxed-melting of the mantle (promoted by the addition of water and fertile material from the subducted crust) results in the formation of basalts and andesites. These mafic melts may differentiate and produce large granitoid batholiths (Annen et al., 2006; Ulmer et al., 2008; Jagoutz, 2010; Jagoutz et al., 2011; Nandedkar et al., 2014). In contrast, large volumes of granitic magmas derived essentially from melting of pre-existing crustal lithologies (Chappell et al., 2000; Collins, 2002; Clemens, 2003; Miller et al., 2003; Chelle-Michou et al., 2015; Laurent et al., 2015), in particular meta-sedimentary rocks that are the most fertile ones, are produced in continental collision settings, owing to crustal thickening and heating after accumulation of heat-producing elements (England and Thompson, 1984; Bea, 2012) and/or high heat flux through the Moho (Depine et al., 2008). Therefore, in a crustal growth perspective, subduction settings (i.e., sites with mostly recycling of the lower plate crust) are apparently favorable settings for the formation of new continental crust, whereas collisional orogens (i.e. sites dominated by tectonic accretion of the lower plate crust) would be preferential sites for its reworking (Cawood et al., 2009; 2013). Again, in each individual convergent segment both processes occur, in variable proportions.

This view, however, only holds when considering short term evolution (i.e. at a time scale similar to the duration of magmatic systems). Recent studies demonstrated that “pure” subduction (following the previous terminology) environments are not efficient sites of long-term crustal growth, because the material extracted from the mantle to build up magmatic arcs is readily recycled in the mantle through subduction of sediments derived from it and/or subduction erosion (Clift and Vannucchi, 2004; Scholl and von Huene, 2007; Scholl and von Huene, 2009; Replumaz et al., 2010; Stern, 2011; Vanderhaeghe and Grabkowiak, 2014). In fact, quantitative estimates demonstrated that the rates of crustal destruction at convergent plate margins is effectively identical to that of new magmatic additions to

the crust, such that the crustal growth is apparently nil (Scholl and von Huene, 2009; Stern, 2011). Furthermore, in the absence of any new magmatic ingrowth of the crust, the whole volume of continents would be recycled back into the mantle within 1.8 Ga (Clift et al., 2009). This is problematic because models of crustal growth through time, especially those based on Hf and O isotope data from the global zircon record, indicate that continental formation occurred continuously (albeit at different rates) since the Hadean (Belousova et al., 2010; Dhuime et al., 2011; Roberts and Spencer, 2014).

Several authors recently proposed that, because of subduction recycling, arc magmatic rocks have a poor preservation potential in the geological record, in contrast with those formed during continental collision that are “shielded” in the core of newly formed (super)continental masses and thus preserved from recycling in the mantle at its leading edges (Hawkesworth et al., 2009; Santosh et al., 2009; Hawkesworth et al., 2010). Moreover, several studies highlighted that formation of new continental crust could also take place in collision settings through fractionation of magmas derived from the mantle (Laurent et al., 2013; Couzinié et al., 2015a, b). As a result, the high preservation potential of small volumes of mantle-derived rocks (and their fractionated daughters) formed during collisional orogens could be an alternative, in terms of crustal growth, to the very poor preservation potential of voluminous arc magmas. This leads to a more general discussion on the time-scale of crustal growth. A package of arc rocks corresponds to purely mantle-derived material. Should it be mostly subducted however, it does not contribute to long term formation of continental crust. Conversely, hybrid rocks partly mantle-derived may represent minor short-term additions to the crust, but be nevertheless much more important long term contributors. As a result, long-term crustal growth does not necessarily superpose with the dominant source (mantle or crust) of an igneous rock.

Moreover, classical tools used as key evidence to address granite petrogenesis, such as trace element patterns and radiogenic isotopes of lithophile elements (Rb-Sr, Sm-Nd, Pb-Pb, Lu-Hf...) provide, in fact, ambiguous information. In the case of mixed sources (involving, for instance, mantle contaminated by crustal material), the incompatible elements signature of such hybrid melts will be controlled to a large extent by the minor crustal component, thus obscuring the volumetrically dominant contribution of the mantle (Laurent and Zeh, 2015; Couzinié et al., 2015a, 2015b). As a result, any attempt, based on isotopes or trace elements, to quantify the balance between crust formation and reworking for a given magmatic rock is vain unless its petrogenesis has been carefully addressed (e.g. Roberts and Spencer, 2014; Laurent and Zeh 2015). Therefore, a complementary approach is required to identify the nature of the source and petrogenetic mechanisms of magmatic suites, prior to any consideration about whether they contribute to crustal growth or not.

Finally, the problem is even more complex when ancient, rather than modern rocks are considered. The tectonic environment in the early Earth (Hadean, Archaean, early Proterozoic) is still poorly

understood – plate tectonics probably operated differently (van Hunen and Moyen, 2012), if at all (Hamilton, 1998; Stern, 2008; Bédard et al., 2012). In any case, subduction was probably not stable at that time (Sizova et al., 2010; Moyen and van Hunen, 2012; Sizova et al., 2014). Therefore, although the Archaean would represent a period of important crustal growth (e.g. Dhuime et al., 2011), translating models developed for the modern Earth to this period is not straightforward.

In this paper, we explore the role of collision-related magmatism in crustal growth. Orogenic belts contain a great diversity of magmatic rocks: linking this diversity to different processes and, importantly, sources – and therefore to crustal growth or recycling – is a challenge. For each type of rock, it is important to assess its source and mode of formation; the meaning of its isotopic signature can only be understood in this light. We firstly describe the petrology and petrogenesis of a granitic province dominated by late-collision granites and thus reflecting the process that occurs when the lower plate crust is fully decoupled from its lithospheric mantle, the eastern part of the Variscan French Massif Central (FMC). There, we decipher the relative contribution of the mantle and the crust based on a composite approach, using not only new isotopic data, but the whole range of available major and trace elements results, used to constrain petrogenetic mechanisms.. This paper is part of a series of contributions with the aim of describing the geochronology (Couzinié et al., 2014, 2015a, 2015b; Chelle-Michou et al., 2015; Mintrone, 2015; Laurent et al., 2015), geodynamic setting (Vanderhaeghe et al., 2014) and isotopic signatures (Couzinié et al., in 2015a, 2015b) of anatexis and granitic magmatism in the FMC, and we refer the reader to these publications for details on these topics. Subsequently, we compare this system to the other end-member system, an oceanic arc with no tectonic accretion, using the well-understood Kohistan paleo-arc as an example. Finally, we explore the implications of this comparison for crustal growth processes and the tectonic setting in which they took place – modern and ancient.

## **2 Granitic magmatism in a (late) orogenic province: the French Massif Central**

### **2.1 Geological setting**

#### *2.1.1 The Variscan belt*

The Variscan belt (Fig. 1a) is a late-Palaeozoic orogenic belt, extending from the Appalachians to the West, to Central Europe to the East. It forms most of the basement of Western Europe, covered by Mesozoic basins and affected by structures related to the Alpine cycle (Matte, 1986). The Variscan belt results from the collision between Gondwana and/or Gondwana-derived microcontinents to the South, and Laurussia—Avalonia to the North (Stampfli et al., 2002; Stampfli et al., 2013). Several intervening (oceanic) basins along the northern margin of Gondwana opened mostly during the

Ordovician (ca. 500—450 Ma) and were subducted in the Silurian to Devonian (420 – 360 Ma) (Bosse et al., 2000; Matte et al., 2001). The subduction provides the first record of convergence between Gondwana and Laurussia. Collision proper occurred during the Carboniferous (350—320 Ma) and was followed during the Upper Carboniferous (320 – 300 Ma) by a phase of exhumation of the lower crust and extensional, late orogenic collapse (Gardien et al. 1997). Between 360 and 300 Ma, volumetric granites were emplaced throughout the belt and represent crustal produced during the tectono-metamorphic evolution of the Variscan belt (Ribeiro et al., 1990; Janoušek et al., 1997; Eguiluz et al., 2000; Ledru et al., 2001; Faure et al., 2009a; Ballèvre et al., 2014; Lardeaux et al., 2014; Žák et al., 2014); etc.).

The core of the orogenic system, the “Moldanubian zone” (Ballèvre et al., 2014), extends from the Bohemian Massif in the East, to the Black Forest and Vosges, to fragments in the Alpine belt, the French Massif Central, southern Armorica and North-Western Spain (the Galicia—Tres Montes Zone). In France and Spain, this zone corresponds to a complex of mostly south-verging allochthonous nappes that include ophiolitic remains (Lasnier, 1971; Burg et al., 1984; Arenas et al., 2007; Schulmann et al., 2014), high-pressure to ultra-high pressure relicts (Gardien et al., 1990; Lardeaux et al., 2001; Berger et al., 2010; Kotková et al., 2011), and overall high grade (upper amphibolite to granulite facies) rocks (Lardeaux et al., 2014). To the south, metamorphic nappes of the Moldanubian zone are thrust over the para-autochthonous to autochthonous terranes representing the northern passive margin of Gondwana. Its northern contact with a variety of terrains along strike is generally obscured or reworked by late transcurrent shear zones.

### 2.1.2 *The Eastern French Massif Central*

The French Massif Central (FMC) is a large (ca. 100,000 km<sup>2</sup>; Fig. 1b) inlier of the Moldanubian zone in Central France. It has been rifted, uplifted and partially covered by lavas during the Cenozoic era (as part of the West European Rift system; Merle and Michon, 2001). The eastern part of the FMC (E-FMC) refers to the terrains located east of the “Sillon Houiller” (“coal line”), a lithospheric-scale strike-slip fault flanked by several pull-apart, coal-bearing Carboniferous basins (Burg et al., 1990; They et al., 2009). The Limousin domain occurs West of the Sillon Houiller, and although its geological history is similar until ca. 320 Ma, it does not expose large migmatite domes such as the ones that are a defining feature of the E-FMC (Vanderhaeghe et al., 2014).

Four main tectono-metamorphic units are commonly identified in the FMC (Burg and Matte, 1978; Burg et al., 1984; Ledru et al., 1989; Faure et al., 2009a; Lardeaux et al., 2014), from the bottom to the top (and South to North): (1) A para-autochthonous unit made of low grade schists and paragneisses (“Schistes des Cévennes” and equivalent units); (2) An amphibolite facies unit of interleaved ortho- and para-gneisses, the “lower gneiss unit” (LGU). In the E-FMC the LGU pervasively melted during the late Carboniferous, resulting in the development of a large, granite-cored anatectic complex, the

Velay Dome (Lagarde et al., 1994; Ledru et al., 2001). The development of the Velay Dome was accompanied by extensional tectonics (Malavieille et al., 1990), detachments driving the exhumation of the dome and, at the upper crustal levels, development of grabens and half-grabens filled by Upper Carboniferous (Stephanian) clastic and coal-bearing sediments in intramontane basins (Becq-Giraudon et al., 1996); (3) An amphibolite facies unit of mostly orthogneisses, the “upper gneiss unit” (UGU) with characteristic relicts of high pressure conditions (granulitic, eclogitic). The base of the UGU is marked by a bimodal magmatic association (amphibolites and meta-rhyolites or granites), locally known as the “leptyno-amphibolic complex” (LAC), that likely represents remnants of an Ordovician oceanic basin or a hyper-extended continental margin (Forestier, 1963; Dubuisson et al., 1989; Pin, 1990). Within and immediately below the LAC, remnants of high pressure metamorphic rocks (eclogites) as well as boudins of mantle peridotite are found (Bernard-Griffiths and Jahn, 1981; Gardien et al., 1990). (4) Epizonal units such as the Brévenne unit, interpreted as a Devonian back-arc association (Bébién, 1971; Sider and Ohnenstetter, 1986). The nappe stack has been intruded by numerous granitic plutons which emplaced mostly from the Lower to the Upper Carboniferous (Laurent et al., 2015) (Fig. 1b).

In a companion paper (Laurent et al., 2015), we present the results of U—Pb dating of 33 samples of granites and associated mafic rocks (vaugnerites) from the Massif Central. We show that (i) granite magmatism in the E-FMC occurred from ca. 340 to 300 Ma with a clear age progression from the North (ca. 340 Ma) to the south (ca. 300 Ma). At ca. 305 Ma, the fast exhumation of the partially molten lower crust resulted in the formation of the Velay dome that locally cuts or includes enclaves of the previously formed granites. (ii) the granitic magmatism is accompanied by minor volumes of mafic magmas (diorites) showing the same spatio-temporal southward migration.

## 2.2 Petrology and geochemistry of FMC granitoids

A large amount of whole rock geochemical analyses were performed in the Massif Central during the 1970's to 1990's in association with the publication of the 1/50 000 geological maps of France (<http://editions.brgm.fr/preCarte50.do>), as well as exploration for Uranium in several portions of the massif. However, this information is disseminated in a large number of reports, articles and fragmentary databases. For this study, we compiled a comprehensive database of published Sr—Nd isotopes (> 450 analyses, including > 220 for granites, but only a fraction including both Sr and Nd isotopic compositions); and whole rock analyses, including major elements (> 2000 samples) and, for part of the dataset, trace elements (> 400 analyses). Finally, U—Pb zircon geochronology, generated by our group, is available for ca. 50 samples of granites, associated mafic rocks and migmatites (Couzinié et al., 2014, 2015a, 2015b; Chelle-Michou et al., 2015; Laurent et al., 2015; Mintrone, 2015).

In this work, we complemented this database with new zircon Hf isotope data from 12 samples of granite from the E-FMC (2 of which –TN01 and TN09— were already reported in Chelle-Michou et al., 2015). In the following, we use this large database in combination with experimental, geochronological, petrological and field arguments to unravel the source of these granitoids.

### 2.2.1 *Main types of granitoids*

The 1/1 000 000 geological map of France (Chantraine et al., 1996) classifies the FMC granites into 4 groups (only three of which occur during the late-collision period in the FMC), essentially similar to those defined by Barbarin (1999):

- (1) Peraluminous leucogranites, equivalent to the Muscovite-bearing Peraluminous Granitoids (MPG) of Barbarin (1999). They are muscovite, or muscovite+biotite bearing; and they are (leuco)granites s.s. in IUGS classification (Streckeisen, 1976). In the FMC, they range from sizeable plutons [uncommonly in the E-FMC, but there are some large bodies in Limousin such as the Millevaches (Faure et al., 2009b; Gébelin et al., 2009) or the Saint-Sylvestre (Holliger et al., 1986) plutons], to small intrusions, dykes or sills concordant with the foliation of surrounding migmatites, and in petrographic continuity with leucosomes in stromatic migmatites (Burg and Vanderhaeghe, 1993). They occur both as “pre-Velay” granites, and as “late migmatitic” bodies cutting across the Velay core complex (Montel and Abdelghaffar, 1993).
- (2) Peraluminous granites to granodiorites, corresponding to the Cordierite-bearing Peraluminous Granitoids (CPG), cordierite ranging from abundant, to rare (Barbey et al., 1999). Texturally they include equigranular (Livradois), to strongly porphyritic (Margeride, Guéret) facies. They are common both in the Limousin and in the E-FMC. In the East, they outcrop both as well defined pre-Velay intrusions cutting across the nappe pile and as enclaves within the Velay complex, or as the heterogeneous granitic phase at the core of the Velay complex, grading into migmatites. Because of its size, specific mode of outcrop and relationship with migmatites, the Velay complex will be treated separately from the other CPG in the rest of this text.
- (3) High-K sub-alkaline granitoids, i.e. K-feldspar porphyritic Calc-alkaline Granitoids (KCG). KCG are, as the name implies, porphyritic granites to granodiorites. They are commonly (but not always) amphibole-bearing, and typically contain abundant accessory minerals such as titanite. They contain micro-granular mafic enclaves (MME: Didier and Barbarin, 1991), and are associated with intermediate to mafic plutonic rocks (diorites, tonalites, monzodiorites) locally called “vaugnerites” (see below). They are scarce in the Limousin, but relatively common in the E-FMC where they form large plutons both North (Saint-Julien la Vêtre, Morvan) and South (Aigoual, Pont de Montvert) of the Velay complex.



### 2.2.2 *Associated intermediate to mafic magmas*

The E-FMC includes ubiquitous, yet small volumes of intermediate, potassic plutonic rocks locally known as “vaugnerites” (Michon, 1987; Sabatier, 1991). Similar rocks are known elsewhere in the Variscan orogen as “durbachites” (Holub, 1997), “redwitzites” (Siebel and Chen, 2009). Elsewhere in other orogenic systems worldwide, they are called “appinites” (Fowler, 1988), “high Sr-Ba granitoids” (Fowler et al., 2008) or “sanukitoids” (Heilimo et al., 2010; Martin et al., 2010; Laurent et al., 2014a), the latter most often in the late-Archaean context. Vaugnerites range from diorite to syenite and consist of amphibole, biotite, clinopyroxene, plagioclase, with variable and subordinate amounts of orthopyroxene, K-feldspar and quartz (Sabatier, 1991). Accessory minerals comprise apatite, allanite, titanite and zircon. Such rocks crop out as meter to decameter-sized rounded to elongated enclaves in granites and migmatites but can also form hectometric sills and dykes of lamprophyric affinity where the magmas are emplaced at higher structural levels (Couzinié et al., 2014). Vaugnerites have a low-silica content ( $44 < \text{SiO}_2 < 63$  wt.%), high FeOt+MgO (10–24 wt.%), Cr (200 – 600 ppm) and Ni (100 – 220 ppm) contents, mg# (molecular Mg/Mg+Fe) higher than 0.65; they also have high K<sub>2</sub>O contents (1.6 – 6.7 wt.% corresponding to high-K to shoshonitic affinities), Ba and Sr (1000–2000 ppm typically; Couzinié et al., 2015a, 2015b). Vaugnerites (or equivalent rocks) are found throughout the Variscan belt (Raumer et al., 2013), but they tend to be ca. 335 Ma old. In contrast, in the E-FMC they occur from ca. 335 to 305 Ma (Laurent et al., 2015). They belong to the larger group of post-collisional mafic magmas, a group of rock that is notoriously difficult to identify based on common “fingerprinting” (Pearce et al. 1984), partly because it was not recognized as a distinct group in classical discriminant diagrams (Ilbeyli et al. 2004). Their petrogenesis is addressed in details in Couzinié et al. (2015a, 2015b).

### 2.2.3 *Whole rock geochemistry and relationships between the different types*

Regardless of their origin, all granitic suites tend to converge towards the eutectic composition (granitic minimum), either because they already result from a minimum melt, or because they evolve (by fractional crystallization) towards the same composition. Therefore, there are many geochemical similarities between all the rocks studied. In the following description, we focus on the main differences between each rock types, as well as on the geochemical link between granites and vaugnerites (the complete whole rock geochemical dataset is provided as Supplementary Electronic item SE1; additional figures can be found in SE2). For granitoids, one of the most critical geochemical indicators is aluminosity, as expressed by indexes such as  $A/\text{CNK} = \text{Al}/(2\text{Ca} + \text{Na} + \text{K})$  (Shand, 1943) or  $A = \text{Al} - (\text{K} + \text{Na} + 2\text{Ca})$  (Debon and Lefort, 1983), both describing the same property. We will show that this feature is the most useful to identify granites having different sources. Other commonly used indicators such as Fe/Mg ratios (Frost et al., 2001) (or Mg#, or similar), K/Na (or equivalently O’Connor (1965) normative feldspar diagram) are not in themselves able to distinguish between granite types. They are however more useful when focusing on differences between otherwise similar

rocks, and to identify smaller differences in sources or processes: for instance the K—Na—Ca systematics is of great use in the Archaean, where a key difference is between sodic and potassic granitoids; and the Fe/Mg ratios have been successfully used to distinguish between different series of arc (Frost et al., 2001), collisional (Debon and Lemmet, 1999; Laurent et al., 2014b) or intra-plate (Dall'Agnol and de Oliveira, 2007) granitoids.

All of the main types of E-FMC granitoids (MPG, CPG, Velay and KCG) are peraluminous (Fig. 2). The vaugnerites, in contrast, are metaluminous. MPG on one hand; KCG and CPG on the other hand plot along parallel arrays in the Shand diagram (A/CNK vs. A/NK), the MPG having lower A/NK, for a given A/CNK, than the CPG and KCG. The Velay granites plot along an oblique array in-between the two trends. In details, the situation varies not only between, but also within each petrographic type and it is possible to identify geochemical sub-types. In the B—A diagram (Debon and Lefort, 1983), using the description of Villaseca et al. (1998), the MPG are “felsic peraluminous”, they are leucocratic and do not define any clear trend. CPG and Velay granitoids are highly to moderately peraluminous (h-P to m-P), with, however, differences between sub-types: the Velay granites show a clear positive trend, the “common” CPG have an ill-defined positive trend and the Margeride CPG (that also have mg# of ca. 60 at SiO<sub>2</sub> = 70 %, compared to 40—45 for the other CPG, see Fig. SE2.1) plots along a flat to weakly negative trend. KCG are moderately peraluminous to metaluminous. Again, there is a difference between magnesian KCG that have a negative trend pointing towards the field of vaugnerites, whereas the more ferroan type shows no clear trend (but extends to higher values of A or A/CNK, overlapping with the field of enclaves and possibly reflecting various degree of hybridization with purely crustal melts).

In terms of trace elements, Rb correlates positively, Sr and Ba negatively with SiO<sub>2</sub> for all granitoid types (Figs. SE2.2 and SE2.3). For a given SiO<sub>2</sub> content, the KCG have higher Sr and Ba values (mirroring the characteristics of the vaugnerites); the Velay granite has lower Rb contents. The MPG show very diverse REE patterns, with LREE ranging from c. 10 times chondritic to c. 100 times chondritic; HREE are slightly less variable. All MPG have a pronounced negative Eu anomaly. The Velay granites also show a large range of LREE and HREE contents, and have a very variable Eu anomaly from markedly negative, to no or even slightly positive anomalies. In contrast, the KCG (although we have less data, and unfortunately only for the magnesian variety) depict much more consistent patterns, with a moderately negative Eu anomaly. The CPG (including the one sample available for the Margeride) are more diverse, but broadly similar to KCG. Finally, the vaugnerites show very diverse, but always high REE values, such that the granites (of all types) are positioned on the low end of the vaugnerites range.

## 2.3 Hf isotopes

### 2.3.1 Methods

Samples were crushed using standard techniques (jaw crusher, disc mill) and sieved to  $<500\ \mu\text{m}$ . Zircons were concentrated using conventional methods (Wilfley table, heavy liquids). After being hand-picked under a binocular microscope, 30 to 100 zircons were mounted on epoxy and subsequently ground and polished to expose their center parts. The internal structures of these grains were characterized by cathodoluminescence (CL) and back-scattered electron (BSE) images prior to analysis using a Jeol JSM-6490 scanning electron microscope (SEM) equipped with a Gatan MiniCL at Goethe University Frankfurt (GUF), Germany.

The results of U—Pb isotopic analyses and corresponding ages for the investigated samples are reported in Laurent et al. (2015). Some of the dated grains were also analysed for Hf isotopes. Hf laser spots were located on top of, or in the same zircon domain (defined on CL/BSE images) as the U—Pb spots.

Hf isotope measurements were performed both on magmatic zircons and on inherited cores at Goethe University of Frankfurt am Main (Germany), using a Thermo-Finnigan Neptune multicollector inductively coupled plasma – mass spectrometer (MC-ICP-MS) attached to a Resolution M-50 193 nm Ar–F excimer laser ablation system, equipped with a two-volume Laurin Technic ablation cell. The latter is fluxed by high-purity, He carrier gas ( $\sim 0.6\ \text{L}\cdot\text{min}^{-1}$ ) and is characterized by rapid response time ( $< 3\ \text{s}$  to get maximum signal strength) and wash-out delay ( $< 5\ \text{s}$  to get  $< 1\%$  of maximum signal strength). Laser spots with diameters of  $40\ \mu\text{m}$  were drilled with repetition rates of  $5.5\ \text{Hz}$  and an energy density of  $\sim 6\ \text{J}\cdot\text{cm}^{-2}$ . Make-up gas consisting of high-purity Ar ( $\sim 0.75\ \text{L}\cdot\text{min}^{-1}$ ) and  $\text{N}_2$  ( $\sim 0.07\ \text{L}\cdot\text{min}^{-1}$ ) was admixed to the carrier gas to improve sensitivity. Post-ablation homogenization is performed by fluxing the gases through a RESOLUTION Instruments Squid® tubing. Data were acquired using multi-collector static mode, during a  $58\ \text{s}$  measurement characterized by  $1.052\ \text{s}$  integration time (55 baseline-corrected ratios).  $^{172}\text{Yb}$ ,  $^{173}\text{Yb}$  and  $^{175}\text{Lu}$  masses were monitored to allow the correction of isobaric interferences ( $^{176}\text{Yb}$  and  $^{176}\text{Lu}$  on  $^{176}\text{Hf}$ ). Instrumental mass bias for Yb isotopes (calculation of  $\beta_{\text{Yb}}$ ) was monitored for each measurement using an exponential law, and corrected to the natural ratio  $^{172}\text{Yb}/^{173}\text{Yb} = 1.35351$ . Mass fractionation of Lu isotopes was assumed identical to that of Yb isotopes ( $\beta_{\text{Lu}} = \beta_{\text{Yb}}$ ), and the average  $\beta_{\text{Hf}}/\beta_{\text{Yb}}$  offset factor estimated during the analytical sessions was about 1.06. The isobaric interferences were subsequently corrected to mass bias-corrected  $^{176}\text{Yb}/^{173}\text{Yb} = 0.79502$  and  $^{176}\text{Lu}/^{175}\text{Lu} = 0.02656$  (see Gerdes and Zeh, 2006). Mass bias for Hf isotopes ( $\beta_{\text{Hf}}$ ) was determined using an exponential law and normalized to  $^{179}\text{Hf}/^{177}\text{Hf} = 0.7325$ . Accuracy and external reproducibility of the method were controlled by repeated analyses of reference zircon standards GJ-1 (Jackson et al., 2004; Morel et al., 2008), Plešovice (Sláma et al., 2008), BB (Santos et al., in press) and 91500 (Wiedenbeck et al., 2004) (see data table SE2 for results). The quoted uncertainties on

$^{176}\text{Hf}/^{177}\text{Hf}$  ratios and  $\varepsilon_{\text{Hf}}(t)$  are quadratic additions of within-run precision of each measurement with the external reproducibility ( $2\sigma$  S.D.) of the reference zircon standard GJ-1 (~70 ppm, see data table). Data reduction was carried out using an in-house MS Excel© spreadsheet (Gerdes and Zeh, 2006; Gerdes and Zeh, 2009).

Calculation of initial  $^{176}\text{Hf}/^{177}\text{Hf}$  ratios were performed using the individual  $^{176}\text{Lu}/^{177}\text{Hf}$  ratio of each measurement, a decay constant of  $\lambda^{176}\text{Lu} = 1.867 \times 10^{-11}$  (Scherer et al., 2001; Söderlund et al., 2004) and the U–Pb age obtained in the same domain of each grain. For the calculation of the  $\varepsilon_{\text{Hf}}(t)$ , parameters of the chondritic uniform reservoir (CHUR) recommended by Bouvier et al. (2008) were used ( $^{176}\text{Lu}/^{177}\text{Hf} = 0.0336$ ;  $^{176}\text{Hf}/^{177}\text{Hf} = 0.282785$ ). Two-step depleted mantle (DM) Hf model ages (TDM2) were calculated using a DM model considering linear regression from present-day depleted mantle as suggested by Griffin et al. (2002), i.e.  $^{176}\text{Lu}/^{177}\text{Hf} = 0.0384$  and  $^{176}\text{Hf}/^{177}\text{Hf} = 0.28325$ , and an average  $^{176}\text{Lu}/^{177}\text{Hf}$  of 0.0113 for the crustal reservoir (Taylor and McLennan, 1995; Wedepohl, 1995).

### 2.3.2 Results

All the analytical results are reported in Supplementary Electronic item SE3. Figure 4 shows the  $\varepsilon_{\text{Hf}}(t)$  – time relationships for all analyses. Combining the Hf data in this work with the published U–Pb data (Couzinié et al., 2014; Laurent et al., 2015), the analyzed samples define two distinct patterns, for CPG, Velay and MPG on one hand, KCG on the other hand.

CPG, Velay and MPG zircon populations are characterized by large proportions of inherited grains (also see Fig. 12a, as well as Laurent et al. 2015). In some samples, most or even all grains are inherited, with only thin (a few  $\mu\text{m}$ ) neo-formed magmatic rims (Couzinié et al., 2014; Laurent et al., 2015). Apart from a few outliers, the magmatic zircons are characterized by  $^{176}\text{Hf}/^{177}\text{Hf}_t$  ratios in the range 0.28260–0.28235 corresponding to subchondritic  $\varepsilon_{\text{Hf}}(t_{\text{emplacement}})$  (from 0 to ca.  $-7$ , with average values for all magmatic zircons in a given sample comprised between  $-4.5$  and  $-2.0$  at the emplacement ages of ca. 300 Ma). The inherited zircons show more scattered Hf isotope compositions, but the main population is characterized by U–Pb ages of 550–530 Ma and  $^{176}\text{Hf}/^{177}\text{Hf}_t$  ratios in the range 0.28250–0.28230 clustered around the chondritic value ( $\varepsilon_{\text{Hf}}(550 \text{ Ma}) = \text{ca. } -3$  to  $+3$ ). Those two dominant populations of inherited and magmatic zircons are linked by an  $\varepsilon_{\text{Hf}}(t)$ –time array requiring an average  $^{176}\text{Lu}/^{177}\text{Hf}$  ratio of ca. 0.01, i.e. close to the average crustal value (ca. 0.0113; Taylor and McLennan, 1985; Wedepohl, 1995). Zircon grains along this trend yield similar model ages of ca. 1.2 Ga. It is worth noting that similar model ages were obtained from bulk rock Sr–Nd isotopes on several FMC granites (Duthou et al., 1984; Pin and Duthou, 1990; Turpin et al., 1990; also see Fig. 7). Some inherited grains show strongly negative  $\varepsilon_{\text{Hf}}(t)$  values (ca.  $-7$  down to  $-27$ ) at any age. Very few analyses, apart from a few inherited zircons, show positive  $\varepsilon_{\text{Hf}}(t)$  values (up to  $+9$ ).

KCG granites mostly lack the inherited zircon component observed in the other granites (see discussion in Laurent et al., 2015). However, their magmatic zircons overlap in Hf isotopic

composition ( $^{176}\text{Hf}/^{177}\text{Hf}_t = 0.28253\text{--}0.28243$ ;  $\epsilon_{\text{Hf}}(305 \text{ Ma}) = -2$  to  $-6$ ) with those of the more crustal, MPG and CPG types. Previously published Nd isotopic data does, in fact show the same pattern: there is no difference in Nd-Hf isotopic data between KCG and CPG-MPG. Furthermore, mafic melts accompanying the KCG (vaugnerites etc.) show the same isotopic signature, both in Hf (Couzinié et al., 2015a, 2015b) and in Sr—Nd systematics (Turpin et al., 1988).

## 2.4 The source of FMC granitoids

Petrogenesis of granitoids results from the superposition of diverse processes such as melting, fractionation, mixing or crystal separation. However, for the purpose of discussing crustal growth, we are chiefly interested in the source of the granitic melts, and less so on the subsequent processes. In this context, the “source” end-members can be either the solid that melts and yields magmas of granitic composition; or the primitive, mafic liquid that fractionates into a granitic liquid. This discussion uses two complementary lines of arguments: first, major elements geochemistry (compared with experimental data); and second, radiogenic isotopes.

### 2.4.1 Major elements: linking granites to their source

Regardless of the process at their origin (melting, fractional crystallization, or even mixing), granitic melts retain some geochemical link with their source (i.e. the rock(s) that melt(s), or the primary liquid(s) that differentiate(s)). From a geochemical point of view, major elements follow mass-balance laws, in all cases, such that they will record the very same chemical relationships during melting, mixing or fractional crystallization. Trace elements do, in theory, follow contrasting laws. However, unless one is looking at very small melt fractions, and/or at elements with very strongly contrasted behaviors, the differences between different processes are relatively minor and not necessarily straightforward to identify (Janoušek et al., 2015). At the scale of a statistically representative dataset (such as we use here), such differences will be definitely drowned in the natural scatter of the data.

This idea may be tested using experimental data. Figure 5 shows the composition of  $> 800$  experimental granitic melts ( $\text{SiO}_2 > 62$  wt. %), generated from sources from basalts to pelites; they are plotted in a  $(\text{Ca}+\text{Al}) - \text{Na}+\text{K}+\text{Al} - 3 \text{Al} + 2 (\text{Na}+\text{K})$  diagram, projected from biotite + quartz +  $\text{H}_2\text{O}$  (See Supplementary Electronic item SE4 for details on the construction of this projection). In this diagram, it is obvious that the nature of the source exerts the main control on the composition of the melt: all liquids from a same source plot along a tight array, pointing to the  $\text{Na} + \text{K} + \text{Al}$  apex (the granite minimum, in this projection) and with a slope that solely depends on the nature of the source. Again, in this context, the nature of the process connecting the source and the granite (melting or crystallization) is irrelevant: equilibrium processes (batch melting or in-situ crystallization) are geochemically identical (this is obvious in an experimental context, and illustrates that there is no way to distinguish crystallization from melting relying on major elements), and fractional crystallization,

although conceptually different, gives actually similar results in this projection as they are both governed by pure mass balance (e.g. Janoušek et al. 2015).

Two lines are important in the diagram of Figure 5: (i) the line connecting the feldspars (horizontal in the figure), corresponding to  $A/CNK = 1$ ; most experimental liquids plot above this line, meaning that all are peraluminous; (ii) the line corresponding to a ratio of 2:1 between the  $3\text{ Al} + 2(\text{Na}+\text{K})$  and the  $(\text{Ca}+\text{Al})$  apices [i.e.  $\text{Al} = 3\text{ Ca} + (\text{Na}+\text{K})$ ]. This line separates liquids connected to a mafic source (basalt or andesite) to liquids connected to felsic sources (meta-granitoids or meta-sediments). As we are projecting from biotite, this line corresponds to no specific  $A/CNK$  value, but steeper lines tend to correspond to higher  $A/CNK$  values. In Shand (1943) diagram, this line separates series plotting with a negative trend, to series plotting with a positive correlation between  $A/NK$  and  $A/CNK$  (cf. Appendix 3). More than any specific numeric threshold (values of 1.1 or 1.2 are commonly proposed: Chappell and White, 1974), the key parameter is the slope a magmatic series defines in Shand diagram (more on that in SE4).

In this light, it is clear that the FMC granites relate to different sources (Fig. 6). MPG tightly plot along the top side of the diagram. CPG (including Velay and Margeride granites) plot immediately above the  $\text{Al} = 3\text{ Ca} + (\text{Na}+\text{K})$  line. KCG fall on or immediately below this line.

Comparing the actual granites with the melts derived from known compositions (Fig. 5) allows interpreting these trends in terms of likely sources. The trend for actual MPG compositions overlaps with the composition of experimental melts derived from very aluminous sources, such as mature (pelitic) (meta)sedimentary rocks. The CPG trend corresponds to a somewhat less aluminous source richer in feldspar (immature sediment and/or felsic igneous rock). The KCG evolution mimics the trends of experimental melts derived from alkali-rich or calc-alkaline basalts.

#### 2.4.2 *The source and petrogenesis of MPG and CPG granites*

Major elements chemistry of these granites is consistent with a derivation from an aluminous source (either metasediments or meta-igneous). The country rocks of the FMC granites are interlayered orthogneisses and paragneisses (both of Ediacaran to Ordovician age; Duthou et al., 1984; Pin and Duthou, 1990; Melleton et al., 2010; Lardeaux et al., 2014; Chelle-Michou et al., 2015), both being possible sources from a regional as well as petrological point of view.

The model ages of CPG and MPG are ca. 1.2—1.1 Ga for all isotopic systems (Hf: this study; Sr: Duthou et al., 1984; Nd: Turpin et al., 1990). In this case, it is clear that these ages have no geological significance: the records of crustal growth in Northern Gondwana (from which the pre-Variscan basement of the FMC is derived; Nance et al., 1991; Nance and Murphy, 1994; Zeh et al., 2001; Zeh and Gerdes, 2010; Fernández-Suárez et al., 2011; Linnemann et al., 2013) show that new crust was formed principally during the Archaean (3.3 Ga), Paleoproterozoic (1.9–2.1 Ga) and

Neoproterozoic/early Paleozoic (0.5–0.6 Ga) (Block et al., 2016; Kemp et al., 2006; Morag et al., 2011; Zeh and Gerdes, 2010), but not in Mesoproterozoic (Grenville) times. Turpin et al. (1990) proposed that the ca. 1.1 Ga model ages do actually reflect mixing between an old (Archaean or Paleoproterozoic) component, and a Neoproterozoic/Panafrican (ca. 0.5–0.6 Ga) juvenile component. The physical mechanism of this mixing would be related to the Cadomian orogenic event, with the formation of plutonic rocks incorporating both old crust, and juvenile magmas. This is consistent with the data from inherited zircons in both granitoids (Laurent et al., 2015) and gneisses (Chelle-Michou et al., 2015) of the FMC, dominated by a Panafrican peak and a “tail” towards older ages; as well as scattered and dominantly negative  $\epsilon_{\text{Hf}}(t)$  prior to 550 Ma (from  $-5$  down to  $-27$ ) and more homogeneous and chondritic  $\epsilon_{\text{Hf}}(t)$  at 550–530 Ma (Fig. 4), suggesting that this ‘mixing’ (deduced from Variscan granites) took place during the Cadomian orogeny. The slightly subchondritic Hf isotope composition of magmatic zircons in the CPG and MPG indicate that the amount of Paleoproterozoic-Archaean crust was minor compared to juvenile Neoproterozoic crust during the Cadomian mixing process. Both the orthogneisses and the paragneisses of the eastern FMC have Ediacarian to Ordovician protoliths, respectively granites and metasedimentary rocks (Duthou et al., 1984; R'Kha Chaham et al., 1990; Chelle-Michou et al., 2015; Mintrone, 2015) related to the Cadomian orogeny, and are therefore isotopically possible sources, as proposed by Laurent et al. (2015) on the basis of inherited zircon age spectra. The large overlap between the isotopic signatures of paragneisses and orthogneisses does not allow a clear discrimination between these rocks (Fig. 7).

To some degree, the major elements chemistry of the granites provides independent answers. The MPG and CPG are chemically distinct (Fig. 6), and probably reflect the involvement of respectively a mature sedimentary, and a quartzo-feldspathic source. In Figure 8, we compare the composition of experimental sources (known to generate liquids of the appropriate compositions) with the composition of FMC basement rocks. Paragneisses and orthogneisses of the LGU feature contrasting compositions (Fig. 8), partly because the orthogneisses happen to be leucocratic and therefore distinctive from the detrital sediments protolith of the paragneisses. Consequently, the paragneisses have compositions similar to the compositions that form MPG-like melts, whereas the orthogneisses are more similar to the potential sources of CPG.

Melting of continental (biotite and/or muscovite bearing) sources has been extensively studied (e.g. Gardien et al., 1995; Stevens et al., 1997; Clemens and Watkins, 2001; Clemens, 2003), and the nature of the resulting melts is also well known (cf. Figure 5, SE4, and references therein).

The MPG granites are “felsic peraluminous” in the terminology of Villaseca et al. (1998) (Fig. 2), and their composition is close to the composition of liquids formed by either water-present or muscovite dehydration melting (similar conclusions were reached for two-mica leucogranites in the Himalayas: Inger and Harris, 1993; Searle et al., 1997; Patiño-Douce and Harris, 1998). At such low melting

temperatures (700 °C), monazite (and zircon) xenocrysts are likely to be preserved through melting reactions (Watson and Harrison, 1984; Montel, 1993), and be physically entrained into the melts. This is confirmed by the abundant zircon xenocryst in these rocks (Laurent et al. 2015). The lack of inherited monazite (Laurent et al. 2015) suggests on the other hand that monazite was subsequently dissolved or re-equilibrated. This results in very variable monazite (and consequently LREE) contents in the granites, and provides an explanation for the huge range in LREE (correlated with Th/U ratios) observed in MPG (more than one order of magnitude: Fig. 3).

The CPG granites extend from the field of experimental melts into the “medium” to “highly peraluminous” fields (Fig. 2), with a weak correlation between A and B parameters. The composition of the mafic components of the suite does not match the composition of experimental melts from crustal sources, unless very high temperatures are considered (> 900 °C: Stevens et al., 2007). Thus, the addition of a mafic component is required. Mixing with a coeval mafic melt is a commonly advocated possibility (Ploquin et al., 1994; Skjerlie and Patiño-Douce, 1995; Patiño-Douce, 1999), but would require a very unusual (high-Al) mafic composition. An elegant solution proposed by (Stevens et al., 2007; Villaros et al., 2009a; Villaros et al., 2009b) is that peritectic cordierite and/or garnet resulting from biotite breakdown reactions would be entrained with the melt into pluton emplacement sites. The resulting magma, a mixture of cordierite (or garnet) and liquid, would have the required mafic and aluminous composition. Biotite breakdown reactions occur at ca. 800–850 °C, and at such temperatures monazite is unlikely to be stable, while zircon can still survive. Thus, LREE behavior is purely controlled by the melt, and therefore more homogeneous (L)REE patterns are observed (Fig. 3).

In summary, we argue that MPG and CPG do result from partial melting of crustal sources. MPG are likely to derive from metasedimentary components (in agreement with zircon xenocrysts showing a wide range age and  $\epsilon_{\text{Hf}}(t)$ ) and CPG from Ediacaran orthogneisses (in agreement with the very limited age-Hf isotope range of inherited zircons). Their isotopic similarity is a result of their derivation from the same crustal segment, and ultimately from a similar material (the Ediacaran sediments deposited on the North Gondwana margin, some of which being reworked in Cambrian to Ordovician to form orthogneisses). Melting occurred at lower temperatures for MPG than for CPG, resulting in more leucocratic magmas carrying variable amounts of inherited monazite in the first case. The fact that the MPG source melted at lower temperatures could either correspond to slightly different compositions (muscovite bearing metasediments, for the MPG, melt at lower temperatures than quartzo-feldspathic gneisses for CPG); or to different fluid regimes (“wet” portions of the crust for MPG allowing lower temperature melting, whereas the source of CPG was dry and could not melt until biotite breakdown).



### 2.4.3 *The source(s) and origin of the Velay heterogeneous granite*

The range of Sr—Nd isotopic compositions for the Velay heterogeneous granite (Williamson et al., 1992; Fig. 7) covers the whole range of compositions observed for all the FMC granitoids. This is also observed (somewhat less clearly) in Mg# values and Sr or Rb contents (Appendices SE1, SE2).

The zircon inheritance pattern in the Velay heterogeneous granite is equally complex. In the eastern and central portions of the dome, Chelle-Michou et al. (2015) and Laurent et al. (2015), respectively showed that the inherited population is dominated by a narrow Ediacaran peak, of the same age as the LGU orthogneisses. In contrast, some of the Velay samples studied by Couzinié et al. (2014) in the South of the dome show a complex population lacking well-defined peaks, more reminiscent of a metasedimentary source akin to LGU paragneisses.

The Velay is a migmatitic dome (Dupraz and Didier, 1988; Burg and Vanderhaeghe, 1993; Ledru et al., 2001); granites proper are poorly separated from their sources, and most of the core of the dome exposes diatexites, equivalent to heterogeneous granites, including large enclaves of metatexites and resisters (Ledru et al., 2001). This enables an investigation of both the actual nature of the source, and the melting reactions involved: a range of lithologies are interleaved and melt at the same time (Weber and Barbey, 1986; Montel et al., 1992; Barbey et al., 2015), under biotite breakdown conditions (ca. 820 °C in this case). In these source zones, liquid-source separation is not fully achieved and this is reflected in the chemistry of the granites. In B—A diagram, Velay granites display positive correlations (i.e. more mafic compositions are also more aluminous) and reach the “highly peraluminous” field of Villaseca et al. (1998): this can be interpreted as poor separation from the restite (or unmolten portions of the source; Chappell et al., 1987; Clarke et al., 2007). Likewise, REE patterns are rather variable (Fig. 3). In particular, Eu anomalies range from slightly positive to strongly negative, again consistent with the entrainment of variable amounts of plagioclase-rich restites (Williamson et al., 1992).

Therefore, the Velay complex is interpreted to represent the root zone of CPG: melt (plus or minus entrained peritectic minerals) extracted from such source zones resulted in CPG plutons, whereas in the Velay complex the whole of the source zone itself (migmatitic para- and orthogneisses) was exhumed during late Carboniferous orogenic collapse.

### 2.4.4 *The source of KCG granites and associated mafic melts*

The nearly total lack of zircon inheritance for high Zr contents in KCG granites suggests crystallization from hot magmas, with minimum temperatures of 850 to 900 °C (Laurent et al., 2015); this contrasts with CPG and MPG having maximum temperatures of ca. 800 °C (and slightly hotter, ca. 820 °C, for the Velay). This makes a purely crustal origin unlikely for the KCG. In addition, they contain ubiquitous comagmatic enclaves (MME) and small bodies of potassic, mafic magmas (“vaugnerites”) (ca. 55 % SiO<sub>2</sub>), for which an origin by crustal melting is impossible (Solgadi et al.,

2007; Couzinié et al., 2014; Couzinié et al., 2015a, 2015b). In isotopic terms, KCG and vaugnerites have the same “crustal” signature, with Hf—Nd model ages of ca. 1.2 Ga, as the CPG and MPG (Fig. 4; Fig. 7). Crust-like isotopic signatures are actually a common feature of all the potassic, mafic late orogenic magmas from Archaean to present (Bonin, 1990; Janoušek et al., 1997; Moyen et al., 2001; Bonin, 2004; Fowler et al., 2008; Heilimo et al., 2010; Janoušek et al., 2010; Martin et al., 2010; Laurent et al., 2014b; Laurent and Zeh, 2015; Couzinié et al., 2015a, 2015b).

Major elements show that the KCG could have an alkali-rich mafic source (Fig. 6), similar to vaugnerites. Figure 8 confirms the similarity between these rocks, and the experimental sources required to explain KCG compositions. The actual differentiation processes could be classical fractional crystallization, or remelting of early underplated mafic magmatic rocks (Laurent et al., 2013) or a combination thereof (MASH processes in deep hot zones: Hildreth and Moorbath, 1988; Annen et al., 2006).

The petrogenesis of vaugnerites is described in details in Couzinié et al. (2015a, 2015b). These authors emphasize that the peculiar geochemical (richness in both compatible and incompatible elements) and isotopic (“crust-like”) signatures can be reconciled by melting of mantle domains contaminated by crustal materials (fluids, melts, or even mechanically admixed felsic rocks *mélange*), as concluded by most studies over the past 20 years (e.g. Bonin, 2004; Conceição and Green, 2004; Condamine and Médard, 2014; Fowler et al., 1997; Heilimo et al., 2010; Holub, 1997; Janousek et al., 2000, 2010; Laurent et al. 2012, 2014b; Martin et al., 2010; Moyen et al. 2001; Rapp et al., 1999, 2010; Scarrow et al., 2009, 2011; etc.). The nature of this crustal contaminant(s) and the way it was incorporated in the mantle are less constrained. In any case, melting of the resulting modified mantle generates magnesian and potassic melts at c. 50-60 % SiO<sub>2</sub>, very similar to vaugnerites, as demonstrated by experimental studies (Rapp et al., 1999; Conceicao and Green, 2004; Rapp et al., 2010; Condamine and Médard, 2014).

The Sr-Nd-Hf isotopic data does not provide any insight on Rb/Sr, Sm/Nd or Lu/Hf ratios in the source. Indeed, several lines of evidence suggest that incorporation of crustal materials in the mantle via subduction and subsequent melting of the mixed domains likely take place during the same orogenic event (within 50 Myr). Therefore, the isotopic signatures result from mixing between materials with contrasted isotopic compositions and does not originate from long-term changes in Rb/Sr or Sm/Nd ratios in the mantle source (see details in Couzinié et al., 2015a, 2015b).

In that respect the isotopic similarity between KCG and CPG (and indeed all other granites) is not coincidental. Rather, it reflects the fact that the bulk of the Nd or Hf budget (both incompatible elements) in vaugnerites (or similar mafic melts) is controlled by the limited amount of crustal rocks that were admixed in the mantle prior to melting and generation of vaugnerite magmas (Couzinié et al., 2015a, 2015b). The isotopic signature of these mafic magmas and their derivatives (KCG) suggest

that this crustal material comes, ultimately, from the same crustal component that also generated the CPG and MPG granites. The same holds, to a lesser degree, for trace elements signatures (Rapp et al., 2010; Marschall and Schumacher, 2012), that are also largely carried over from the contaminant, to the mafic melts, to the granitoids.

In summary, our preferred model for KCG is by differentiation of a mafic (vaugneritic) melt, itself the product of melting of a mantle enriched by a component ultimately derived from an ancient crust. This crust was very similar to the crustal source of CPG and MPG, i.e. isotopically homogenized Cadomian granitoids.

### **3 Granitic magmatism in a supra-subduction arc: the Kohistan batholith**

Melting of supra-subduction mantle wedge (and the formation of magmatic arcs) is the other important mechanism of granite genesis on Earth, and supposedly one of the main contributors to crustal growth. In this section we compare the main features of granitic magmatism in both major granite-forming systems on Earth: magmatic arcs, and post-collision zones. In simple terms, the opposition between arc and post-collisional zones also overlaps with the age-old debate on the origin of granitic rocks, by (i) partial melting of older crust or (ii) differentiation of (arc) basaltic melts. In light of the considerations presented above (section 2.4.1), the chief difference is one of source (felsic vs. basaltic lithologies).

As an example of magmatic-arc related granitoids, we will focus on the Kohistan island arc in Pakistan, that has been extensively studied in the recent years, and for which a dataset consistent in scope and details with the one presented here for the FMC is available (Dhuime et al., 2009; Jagoutz et al., 2009; Jagoutz, 2010; Bouilhol et al., 2011; Bouilhol et al., 2013). The Kohistan arc represents an end-member situation with no crustal reworking, corresponding to a system where the lower plate crust is fully coupled with the lithosphere and totally recycled into the mantle. It does therefore strongly contrast with the FMC, and both case together define the extreme situations between which a range of possible cases may occur.

#### **3.1 Geological setting and petrology**

The Kohistan arc (Fig. 9; Jagoutz et al., 2011) is a fossil Jurassic to Cretaceous oceanic arc that is now part of the Himalayan belt. The Southern portion represents a mafic lower (to middle) arc crust, with rare occurrence of mantle rocks (Jijal and Sapat complexes). The Northern portion is occupied by the Kohistan batholith. The batholith has not been mapped in details but is composed of multiple intrusions (Debon et al., 1987; Crawford and Searle, 1992) that range from gabbro, to diorites,

tonalites, granodiorites and leucogranites, defining a complete differentiation series (Jagoutz et al., 2009; Jagoutz, 2010).

### 3.2 Major and trace elements

In terms of major elements (as captured by the projection from biotite described in this paper), the Kohistan arc granitoids do strongly differ from all the FMC granitoids (Fig. 10). In the triangular projection, they define a nearly horizontal trend along the  $A/CNK = 1$  line (Fig. 10c), which corresponds to the compositional evolution of liquids derived from experimental differentiation of tholeiitic or mildly calc-alkaline basalts and intermediate rocks (Fig. 5). As such, they differ from KCG by the nature of the fractionating mafic material, which is much richer in alkalis and poorer in CaO in the case of KCG (Fig. 8)

Importantly, the real discriminant factor is not so much the composition of one individual sample, but the shape of the whole trend defined by each suite. Owing to the existence of a granitic minimum (eutectic), that will correspond either to the composition of the first minimum liquid during partial melting, or to the last drop of residual liquid at the ultimate stage of differentiation, every suite will feature samples with similar compositions – leucocratic, and mildly peraluminous. In itself, the presence of peraluminous samples in a suite is therefore no proof for crust involvement. However, the different types of granitoid suites reach this composition via different pathways: in Shand (1943) diagram (Fig. 10), the minimum at  $A/NK \approx 1$  and  $A/CNK \geq 1$  is reached in the Kohistan arc through an array with a steep negative slope, extending from high  $A/NK$  and low  $A/CNK$  values, whereas the low-Ca S-type plutons rather show an array with a positive slope and  $A/NK \approx A/CNK$ . Similar features are observed in the B—A diagram, and in the triangular projection from biotite defined above.

On the scale of a whole crustal segment, this approach therefore appears to best capture the differences between regions where the main source of granitoids is a mafic arc-like magma (arc situations s.l., defining trends with mildly positive slopes in the triangular projection), and regions where the source is the pre-existing crust (collisions, defining trends with clear negative slopes). This confirms the importance, on a planetary scale, of two main granite-forming systems with contrasting behaviors.

Trace elements are of marginal use in this context. The REE patterns for both FMC granitoids (Fig. 3), and Kohistan rocks (Fig. 11) are very similar (apart from some Kohistan rocks having steeper REE patterns). Several factors contribute to this result:

Firstly, from simple geochemical laws such as batch melting or fractional crystallization equations (Shaw, 2006; Janoušek et al., 2015), it follows that the composition of a melt depends both on the source and the mineral phases involved during melting and/or fractionation. Amongst the major minerals in equilibrium with a felsic melt, very few have high partition coefficients and thus the potential to shape the trace elements patterns: garnet (perhaps amphibole) and plagioclase are the most

influential players. Plagioclase is present at some point during the history of all granites; the presence or absence of garnet probably accounts for the steeper Kohistan REE patterns (Jagoutz, 2010).

The trace elements compositions of the sources involved are not massively different: in the case of an arc system, the source was an arc basalt. In the case of a post-collision environment, the dominant contribution to the (incompatible) trace elements budget is the pre-existing continental crust, whose bulk composition is similar to arc rocks (Rudnick and Gao, 2003).

Secondly, many trace elements (REE in particular) are controlled primarily by accessory minerals in felsic melts (Bea et al., 1996). Although the nature of the minerals may differ (monazite in peraluminous magmas vs. allanite in metaluminous ones), the net result is that the REE budget reflects primarily equilibrium with accessory minerals, and preserves little information on the source or the major minerals.

Therefore, within the natural scatter of statistically representative datasets, there are no reasons for arc magmas to be strikingly distinct from late-collision rocks in terms of their trace elements composition.

### 3.3 U—Pb and Hf isotopes in zircons

The Hf isotope-age patterns in zircons are in sharp contrast between convergent plate margins and sites of continental collision. Crust-derived granites of the FMC show a sizeable proportion of inherited zircons (ca. 35% in average, but up to 50-75% for the MPG and Velay heterogeneous granites). In some samples, no magmatic grains were found, and only small rims may be interpreted as magmatic (Couzinié et al., 2014; Laurent et al. 2015). On the other hand, KCG (and vaugnerites: Couzinié et al., 2014, 2015a, 2015b) contain mostly magmatic grains, with no, or very rare, inheritance. A similar pattern is found in all Kohistan granitoids (Bouilhol et al., 2013), and associated mafic rocks (Bosch et al., 2011). However, whereas all Kohistan granitoids feature a juvenile ( $\epsilon_{\text{Hf}}(t) \approx +10$ ) isotopic signature, all granitoids of the FMC, comprising crust-derived granitoids (MPG, CPG, Velay) as well as mantle-derived KCG and vaugnerites reveal exclusively chondritic to subchondritic Hf isotopic compositions (Fig. 12).

Therefore, the combination of the age (inheritance) and isotopic (DM vs. crust like) patterns, taken together, offer a very potent means to discriminate between the two kinds of environments, and confirm the petrological and geochemical observations. Specifically, the age (inheritance) patterns allow to distinguish between dominant sources (crust vs. mantle), whereas the Hf isotopic patterns discriminate between the type of mantle involved, and thus to some degree between geodynamic sites.

In terms of crustal petrogenetic processes, we demonstrated that both Kohistan granitoids and KCG correspond to similar petrogenetic process, namely differentiation of mantle-derived material, although the latter has different characteristics in the two settings. The contrasting  $\epsilon_{\text{Hf}}(t)$  patterns

indicate that in the case of the Kohistan, new (mantle-sourced) Hf was added to the crust; whereas in the FMC, new material was added, but no (or very little) new Hf. This mainly reflects the fact that the Kohistan granitoids were generated in an oceanic island arc, away from any pre-existing continent, whereas the KCG of the eastern FMC formed within an already mature continental environment, such that the whole Hf budget is controlled by non-radiogenic Hf, due to subduction of materials derived from the existing crust (Laurent and Zeh, 2015; Couzinié et al., 2015a, 2015b). Furthermore, the generation of KCG, as proposed above, might also involve mixing with MPG and CPG.

## 4 Discussion

### 4.1 Bimodal magmatism: a hallmark of delamination in late-collisional environments

Granites in the FMC are mostly post collisional tectonic, cutting across previous structures, and have a dual origin. On one hand, the majority of granites (MPG and CPG, including Velay) correspond to partial melting of preexisting crust. On the other hand, KCG are ultimately formed by differentiation of mantle-derived melts (vaugnerites). Like in other collisional settings of different age worldwide (Bonin 2004; Corfu 2004; Clemens et al. 2009; Frost et al. 2001; Laurent et al. 2014b; Liégeois et al. 1998, etc.), this points to a late-collisional magmatic activity dominated by concurrent melting of both the crust and the mantle (though this mantle has peculiar properties).

This association is distinctive from pre-collision (or subduction) related magmatism, on one hand, which is dominated by mantle-derived magmatism (cf. part 3 above); and from early or peak collision magmatism (Debon et al. 1987; Inger and Harris, 1993; Searle et al., 2010) that is the result of (nearly) pure crustal melting.

Correct interpretation of this environment is critical to tectonic reconstructions. The KCG in particular (or comparable granites in the Variscan belt or worldwide) can easily be misinterpreted: they may be regarded as late-subduction magmas, perhaps contaminated by the crust, or as purely crustal, syn-collision melts (both models accounting for their isotopic signatures, but failing to reproduce their whole-rock geochemistry). Rather, we demonstrate that the key feature is the whole association, including the crustal melts together with the very specific Mg-K magmatism (Scarrow et al., 2009; Scarrow et al., 2011).

Coeval melting of the crust and the mantle is favored in a convergence context with concomitant crustal thickening by tectonic accretion and thinning of the lithospheric mantle owing to slab retreat (Vanderhaeghe and Duchêne, 2010). In the case of the FMC, the evidence is summarized in Vanderhaeghe et al. (2014), including geochronological (Laurent et al., 2015), geophysical (Averbuch and Piromallo, 2012) and paleo-ecological (Becq-Giraudon et al., 1996) arguments. The increase in temperature affecting the orogenic crust leads to partial melting triggering the development of an

orogenic plateau and eventually controlling gravitational collapse of the Variscan belt. Importantly, there is a notable difference between the Eastern part of the FMC, which has been affected by slab removal, and the Western part, that was not. (Averbuch and Piromallo, 2012). The late, bimodal association we describe here occurs in the E-FMC but not in the West (Limousin), where vaugnerites, KCG granites and large, late migmatitic core complexes are missing (Vanderhaeghe et al., 2014). Likewise, the Eastern part of the FMC is marked by quick uplift and exhumation of deep rocks (e.g. clasts of Velay granite in nearly co-eval sedimentary basins; hypovolcanic granites cutting across migmatites of same U—Pb age [Didier et al. 2013]) that is not documented in the Limousin.

The pervasive melting associated with delamination promotes the transfer of incompatible heat producing elements towards the surface, and helps in creating a thermally stable crust. Melting of the underlying orogenic mantle (forming vaugnerites) does at the same time strip the mantle from its incompatible elements, helping in the formation of a depleted, refractory mantle root. Collectively, delamination and its associated magmatic processes therefore appear as a key element in the termination of orogenic systems and the generation of a stable lithosphere.

#### **4.2 Earth's main granite forming systems – a tectono-thermal point of view**

The two systems described in this contribution represent end-members of a range of possible tectonic environments. They provide therefore valuable insights on the way granites are formed along convergent plate boundaries, and allow to speculate on possible intermediate scenarios.

A useful framework to that effect is discussed in Vanderhaeghe and Duchêne (2010). Plate convergence is accommodated by subduction of part of the lithosphere. Two key parameters control end-member scenarios for the structures developed in these environments: (i) coupling vs. decoupling of the crust from the downgoing plate. If the crust is fully coupled to the lithospheric mantle, the system is a subduction zone (oceanic or continental); if the crust and the mantle are decoupled, tectonic accretion of the crust leads to the development of an orogenic wedge. (ii) advance or retreat of the slab. Slab advance promotes thickening of the upper plate (crust and lithospheric mantle) whereas slab retreat results in thinning of the lithospheric mantle of the upper plate.

Situations of crust-mantle coupling result in burial of hydrated rocks from the surface, and thus promote partial fluxed melting of the mantle wedge. On the other hand, slab retreat (and associated lithosphere thinning) will cause asthenospheric upwelling beneath the overriding plate. Combined crust-mantle decoupling and slab retreat results in thickening of the crust and thinning of the lithospheric mantle. Therefore, the 4 scenarios identified by Vanderhaeghe and Duchêne (2010) will result in contrasting granitic systems (Fig. 13a):

- Case A (crust-mantle coupling and slab advance; A1 with oceanic crust, A2 with continental crust) will generate relatively cold environment in the upper plate owing to thickening of the lithospheric mantle, and strong influx of water into the mantle caused by subduction. This will result in the generation of large volumes of melts in the mantle (that may then differentiate into granites), but no or limited crustal melting as the only heat in the system is brought in by the magmas from the subduction (Annen et al., 2006). The Kohistan is a good example of such scenarios.
- Case B (decoupling and slab advance) is less favorable to water addition to the mantle, neither does it allow large-scale melting of the crust. The resulting margin will have very little magmatic activity associated with it. This scenario is usually designated as indentation, with classical examples associated with the India—Eurasia collision.
- Case C (coupling and slab retreat; C1 and C2) generates high geothermal gradients in the upper plate, as well as important water flux into the mantle. As a result, large amounts of both crust and mantle melts can be generated. This scenario might apply to zones of continental subduction such as invoked for the Pyrenees (Vanderhaeghe and Grabkowiak, 2014) or for the Western Gneiss region in the Caledonides in Norway (Labrousse et al., 2011).
- Case D (decoupling and slab retreat) is the scenario the most favorable to crustal melting, as it generates thick, hot crustal environments in the overriding plate. Mantle melting is however less likely, at least in this steady-state situation. In absence of enrichment of the overriding plate by the subducted slab, the lithospheric mantle in the upper plate is less prone to melt, although decompression melting of the (less fertile) asthenosphere remains possible. The Aegean, with migmatites and a variety of magmatic rocks encompassing tholeiitic basalts, calc-alkaline granites and peraluminous leucogranites emplaced in the upper plate of the southward retreating Hellenic slab, is probably the best example of such a scenario (Vanderhaeghe, 2004; PePiper and PePiper, 2006; Kruckenberg et al., 2011; Menant et al., 2016). Another example is the Songpan Ganze terrane in the central part of Tibet, which corresponds to a huge accretionary wedge made of turbidites intruded by a alkaline, calc-alkaline and peraluminous granitoids (de Sigoyer et al., 2014).

None of these situations is, however, steady-state, and the influence of the pre-existing situation is critical. Old subduction zones (coupling of the crust to the down-going mantle slab) allow the introduction of crustal material in the mantle, and make it more prone to subsequent melting. Thickening of the heat-producing crust (slab advance or crust-mantle decoupling) allows heat accumulation (England and Thompson, 1984). Fig. 13(b and c) outline two possible evolving situations. (b) features a classical subduction—collision cycle, with an initially advancing and coupled plate boundary with a subduction and the development of a magmatic arc; followed by collision (decoupling of the crust) and little magmatic activity; and eventually slab retreat (similar to the FMC



described here). During the first stage, subduction promotes mantle enrichment; during the second stage, crustal thickening favors crustal heating, such that the final stage results in abundant magmatism, derived both from the crust and the mantle. (c) is an example of an active continental margin with alternating phases of slab advance and slab retreat (Collins, 2002; DeCelles et al., 2009), over a well-coupled (oceanic) crust. In this scenario, the mantle flux is important throughout. Crustal thickening during the advancing stages favors melting during the retreating periods.

Obviously, many other scenarios are possible. However, the end-members described here provide a conceptual framework to discuss their evolution.

### 4.3 Contributions to crustal growth

#### 4.3.1 *Crustal growth in late orogenic sites*

The Variscan FMC is a crustal segment dominated by granitic magmatism. A large portion of those granites (MPG and CPG, Velay included) is however purely, or mostly of crustal origin and correspond to crustal recycling, but not to crustal growth. On the other hand, the KCG granites reflect addition of new material to the crust since they derive from fractionation of mantle-derived material. Hereafter, we consider that this process is the hallmark of new crust formation, because it results in net growth of the crustal volume from input of mantle-derived material, regardless of the isotopic signature of the latter (Couzinié et al., 2015a, 2015b). This is a key point, since as we discussed here, the isotopic signature of the KCG is similar to the regional crust. As a result, a purely isotopic approach would regard these rocks as plain reworking, and totally ignore their contribution to crustal growth.

In the case of the KCG magmatism, it is clear that most of the Hf (or the Nd, and probably part of the Sr) ultimately comes from the crust – it has been carried into the mantle, and from there to vaugneritic melts and to granites and eventually back to the crust (Couzinié et al. 2015a, 2015b). There is, therefore, no significant addition of new Hf (and other incompatible elements) to the crust through this process, and most of the Hf in the KCG is old, crustal Hf. On the other hand, all or most of the compatible elements (Mg, Fe, Ni, Cr, etc.) in the vaugnerites, and hence in the KCG, are of mantle origin: they have never been involved in a crust extraction-reworking cycle, in contrary to the incompatible elements. There is, as a result, addition of large amounts of these elements to the crust. Mass balance calculations (Couzinié et al., 2015a, 2015b) demonstrate that 70 to 80 % of the bulk mass of the FMC vaugnerites ultimately comes from the mantle, the old crust component accounting for no more than 20–30 % of the mass. Considering that the KCG result from fractionation of vaugnerites with only limited crustal contamination or mixing with crustal felsic melts, which is besides supported by geochemical modelling on Archaean or Paleozoic analogues; (Fowler and Henney, 1996; Laurent et al. 2013) and the major-element approach presented earlier on (section 2.4.1, Figs. 6 and 8), the KCGs (and vaugnerites) contribute significantly to crustal growth. This

crustal addition is actually totally invisible from an isotopic point of view, since the commonly used isotopic tracers (Sr, Nd, Pb, Hf) are all incompatible elements and therefore fully controlled by the relatively small proportion (<20%) of crustal component recycled into the mantle source (Couzinié et al., 2015a, 2015b).

This emphasizes the point that new additions to the crust cannot be defined from a sole isotopic perspective. Here we have material that is not “juvenile”, from a pure isotopic point of view (i.e. its signature is nowhere near the depleted mantle), but does nevertheless correspond to new crust formation. We suggest that the opposite situation may occur, with purely crustal rocks having an isotopic signal suggesting the involvement of an isotopically juvenile component. For instance, peraluminous, two-mica or cordierite bearing S-type granites may contain zircons with a range of isotopic compositions (Kemp et al. 2009), because they derive from an heterogeneous, and purely crustal, meta-sedimentary source (Villaros et al. 2011).

At the scale of the FMC, KCG are by no means the dominant component but they represent a sizeable amount nonetheless (Fig. 9): in terms of outcrop area, the KCG in the FMC represent ca. 3,500 km<sup>2</sup> (out of a total outcrop surface of 14,000 km<sup>2</sup> of granites), i.e. about 25%. Granites, of course, make up only one third to one half of the total Variscan outcrop. Combining these figures leads to an estimate of ca. 75% (mass fraction of KCG having a mantle origin) × 25 % (proportion of KCG) × 30—50 % (granite outcrop) ≈ 5 to 10 % of juvenile material in the Variscan crust of the FMC. Applying similar figures to the whole of the Variscan belt, where comparable distribution of granitic types are observed (Finger et al., 1997; Janoušek et al., 2000; Scarrow et al., 2009; Raumer et al., 2013), corresponds to large volumes of crustal addition,.

#### 4.3.2 *From juvenile rocks to long-term additions to the crust*

The fact that new crust is extracted from the mantle at a given time does not necessarily mean that it will become a long term addition to the continental crust (Hawkesworth et al. 2009; Cawood et al. 2013). For instance oceanic arcs (such as the Kohistan) are dominated by juvenile rocks, recently extracted from the mantle. However, this does not necessarily translate in long-term crustal growth, because they also are likely to be recycled into the mantle since those environments have poor preservation potential in the geological record (Hawkesworth et al., 2010). This has been for instance recently documented in the Grenville orogeny, where syn-orogenic zircon populations record Hf isotope—age patterns corresponding to the activity of pre-collision arc complexes that are poorly represented in the geological record (Spencer et al., 2015). Likewise, in recent arc settings such as Japan (Isozaki et al., 2010), the study of sedimentary rocks with different deposition ages showed a progressive consumption of successive arc sequences through time by subduction erosion (Stern, 2011). In this perspective, oceanic (or continental) arcs only become permanent additions to the crust if they are accreted against continental masses, which happens in (accretionary) orogens, and

subsequently isolated from further recycling during a collisional orogeny (Condie et al., 2011). In complete contrast, continental collision (and post-collision) sites may be sites of lesser voluminous juvenile magmatism (<10% of the bulk continental mass, on the basis of the FMC example), but the magmas formed in these sites have a very high preservation potential and therefore readily become permanent additions to the continental crust.

A main consequence of this preservation problem is that at the scale of whole orogenic belts (e.g. the Variscan and the Himalayan belts), both systems result in comparable volumes of new addition to the crust. Indeed, whereas the bulk of the mass of Kohistan granitoids is mantle-derived, supra-subduction complexes represent no more than ca. 10% the area of the Himalayan belt (Fig. 9), which is a minimum since some subduction-related material may have been incorporated in pre-orogenic sedimentary sequences subsequently trapped in the collisional belt. In contrast, the Variscan KCG are not the most widespread rock type in the whole orogenic system and are not purely mantle-derived – but they are found throughout the belt, from Spain to the Bohemian Massif (and also in Western Alps, Corsica, Cornwall, etc.) and thus would roughly account for 5 to 10 % of juvenile material in the bulk Variscan crust. This value is also a minimum, since small volumes of magmas related to the waning stages of subduction prior to continental collision proper are present in the MCF, as late Devonian gabbro-tonalite-granodiorite, amphibole-bearing calc-alkaline plutons (“ACG” in the classification of Barbarin, 1999) especially in the Limousin area (Bernard-Griffiths et al., 1985; Pin and Paquette, 2002). Those would also represent new additions to the crustal volume, yet their very subordinate importance in terms of surface (< 2 % of the exposure in the FMC, nearly none in the Eastern FMC) clearly shows that only the final stages of subduction-related magmatism is captured in collisional belts.

In essence, in the Variscan belt, crustal growth is a result of relatively small volumes of mantle derived rocks in a given area, but present throughout the belt and preserved as such. In the Himalayas, the same result is achieved by addition of a handful of purely mantle-derived, small complexes that happened to be preserved and accreted against Asia. The two models are, of course, to be considered as end-member situations in a larger range of scenarios involving diverse proportions of tectonic accretion (and subsequent reworking) vs. magmatic additions from the mantle. However, the key point is that both appear to contribute to long-term crustal growth at the same order of magnitude.

Although this is beyond the scope of this paper, we note that all these issues are further exacerbated when dealing with detrital zircons (for which the petrological context is lost). We demonstrated here that there is no simple way to link an isotopic (Hf, or even O – Couzinié et al. 2015a, 2015b) signature to reworking vs. crustal additions, and that the fact that a magma was extracted from the mantle (and thus potentially sampled in the detrital record) is no proof that it became a long-term component of the crust. This comes on top of the well-known issue of “zircon fertility” (different types of magma will

crystalize different amounts of zircons, such as the proportion of zircon crystalized does not correlate to the volume of rock formed: Cawood et al. 2013). Collectively, all these issues cast serious doubt on the validity of crustal growth models based on out-of-context zircons.

#### 4.4 Archaean crustal growth

Depending on the preferred model, 50 to 100% of the volume of the continental crust was extracted from the mantle during the Archaean (Belousova et al., 2010; Roberts and Spencer, 2014; Taylor and McLennan, 1995; Hawkesworth et al., 2010; Dhuime et al., 2011). However, the (geodynamic) processes operating on the Archaean Earth are not known, and may well have been largely different from those operating today (Hamilton, 1998; Stern, 2008; Bédard et al., 2012). It is therefore difficult or impossible to simply apply models derived on the modern Earth to the Archaean situation.

It has long been recognized that the dominant component of the Archaean crust is a suite of granitoids (tonalite, trondhjemitic and granodiorites), collectively referred to as the TTG suite (Martin, 1994; Moyen and Martin, 2012). Therefore the debate on the genesis of the Archaean crust is largely superposed to the discussion on the petrogenesis of TTGs.

Three main models (or families of models) are proposed for the origin of TTGs and Archaean crustal growth:

- (i) Fractionation of arc basalt into tonalites. This model is mostly implicit, a result from extending models for modern-day crustal growth in arcs into the Archaean (Hawkesworth et al., 2010; Arndt, 2013). However, some petrological studies (Kamber et al., 2002; Kleinhanns et al., 2003) apply this model to individual Archaean suites; or to comparable modern rocks (Davidson et al., 2007; Jagoutz et al., 2011).
- (ii) Melting of metabasalts. This is probably the dominant petrogenetic model for the formation of the TTG suite (see review in Moyen and Martin, 2012), and comes in two geotectonic flavours:
  - a. Melting of a hot, subducted slab (i.e. the “adakitic model”), as described for instance in Martin (1986) and many subsequent publications. In this model, the hotter Archaean mantle is responsible for melting (rather than dehydration) of (meta)basalts in subducted slabs; the Archaean arc magmatism is therefore TTG in nature.
  - b. Melting at the base of a thick oceanic crust (or basaltic plateau) (e.g. Van Kranendonk et al., 2007), or delaminated portions below a plateau (Bédard, 2006). This model is primarily supported by the lack of clear arc-related features (thrust and fold belts, HP-LT metamorphism, tectonic mélange, etc.) in the Archaean geology (Hamilton, 1998; Hamilton, 2003). Its main petrological shortcoming is the difficulty to supply enough water to deep crustal zones without some kind of subduction.

To a point, the paradigm of subduction-related crustal growth did influence the models for the petrogenesis of the Archaean juvenile crust and other alternatives have been less explored. In the light of the discussion of this paper, we speculate on an alternative, and wish to explore the possibility that TTGs (or at least some of them) formed in an environment dominated by partial melting of pre-existing crustal lithologies.

We first apply the logic developed in this paper to discuss the source of TTGs. Their major elements characteristics (Fig. 14) require a source (Na-rich basalts) distinct from arc basalts, as they plot with positive slopes in Shand diagram and negative slopes in the triangular projection developed in this work, unlike the Kohistan granitoids (see Fig. 10). The source of Archaean TTGs is increasingly recognized as being an enriched basalt in elemental and isotopic terms (Adam et al., 2012; Nagel et al., 2012; Martin et al., 2014): not MORBs, but more closely related to material sourced from a deeper, primitive mantle (Guitreau et al., 2012). It is also well-known that O-isotopes in zircons show a marked increase at ca. 2.5 Ga, interpreted as reflecting the increasing role of crustal recycling in the genesis of granitoids (Valley et al., 2005). However, even much before 2.5 Ga, typical  $\delta^{18}\text{O}$  values in zircons (from TTGs) are between +6 and +7, clearly above the mantle value (+5.3) and in good agreement with recycling of surface-weathered material (Zeh et al., 2014). This is in agreement with experiments as the only experimental starting materials that does produce TTG-like melts (Fig. 5; Fig. 14) corresponds to alkali (sodium) rich basalts, similar to seafloor altered rocks (Zamora, 2000).

All these features do not resemble modern subduction-related environments. In addition, there is little in the geological record that allows linking TTGs to fractionating mafic melts. Arc-like mafic rocks are rare in the Archaean, and in any case mafic rocks are rarely coeval with TTGs. Full differentiation series, Kohistan-style, are lacking from the Archaean record. Finally, geodynamic modelling shows that subduction was probably not as stable in the Archaean as it presently is, owing to higher mantle temperatures (Sizova et al., 2010; Moyen and van Hunen, 2012; van Hunen and Moyen, 2012).

Recent numerical modelling of Archaean geodynamics (Sizova et al., 2014) provides a valuable tectonic framework, and alternative petrogenetic model. In this model, an early basaltic crust forms at the top of the mantle, and stays at the surface, in contact with the hydrosphere, for long periods of time. Periodically, this proto-crust is resurfaced by new mafic flows or intrusions. When the proto-crust becomes too thick, its dense base can delaminate and sink into the mantle; as the system cools down and becomes more rigid, the delamination systems evolve into increasingly stable zones of crustal burial, similar to subduction zones, and with a limited, but increasing, potential to drive horizontal mobility (Moyen and van Hunen, 2012) and promote collisions initially between thick segments of the mafic crust, then felsic continental nuclei.

TTGs may form in different places in this system: (i) in the proto-collision zones, through the burial and exhumation of hydrated mafic rocks; (ii) over delamination zones, via a heating mechanism not

unlike the one described in this paper for the FMC; (iii) in delaminated (or proto-subduction zone) units themselves, as they are buried in the mantle (Bédard, 2006). An implication of this model is that melting will occur at different depths, matching the observations of Moyen (2011) on the existence of several distinct TTG suites formed by melting at different depths.

Consequently, we speculate that Archaean TTGs resulted from reworking of an earlier (altered) basaltic protocrust, through a range of processes including delamination, proto-subductions (Martin, 1986) and proto-collisions (Chardon et al., 2009). In this view, they do not contribute to short-term crustal growth (as they all derived from a long-lived mafic protocrust); but they permit the stabilization of crustal nuclei and the long-term preservation, within the crust, of part of the material originally extracted into the mafic protocrust (Laurent and Zeh, 2015). Arc-like granitoids do occur in the Archaean record, but typically late in the evolution of a given crustal segment, when the cratonic lithosphere was mature enough to allow stable subduction beneath it (Laurent et al., 2014a; Laurent and Zeh, 2015).

## 5 Conclusions

Both supra-subduction arcs and late-orogenic domains are sites where large volumes of granitic magmas are formed. These two environments correspond to fundamentally different situations; arc crust forms by differentiation of mafic melts, and the heat available is restricted to what is advected by the melts. The post-orogenic crust is a very hot system, permitting large-scale crustal melting, and granite formation chiefly by melting of the preexisting crust. The hallmark of such late-orogenic sites is a bimodal magmatic activity with the formation of (i) crust-derived granites, either at relatively low temperatures (water present or muscovite breakdown) in lithologies that permit it; or at higher temperatures (biotite breakdown) otherwise. These granites are extracted from a middle to lower crustal partially molten zone (that is locally exposed, in core complex structures, via late-orogenic extensional processes). (ii) mantle-derived Mg-K mafic melts, that evolve into granitoids either through crystallization or melting of recently underplated bodies; the source of these melts is a mantle contaminated by crustal material (introduced during preceding subduction?).

The petrological difference between both sites is a result of contrasting geodynamic environments. Magmatic arcs correspond to strong coupling of the crust with the downgoing slab, favoring the transport of water to mantle depth, and its release triggering mantle melting. In contrast late-orogenic environments reflect retreating plates and lithosphere thinning. Such sites are particularly efficient at forming granites if the slab retreat occurs after a full orogenic cycle involving crustal thickening and mantle enrichment. In such situations however, the amount of melt introduced in the crust from the mantle is significant, such that these sites are an important contributor to crustal growth.

In the Archaean, the difficulty to support long-lived, stable subduction would hinder the development of mature advancing arc systems. The episodic subduction style, that is probably typical from the Archaean Earth, would result in much more common slab retreat, and limited coupling between the subducting slab(s) and the mantle. Consequently, we propose that large portions of the Archaean TTG crust were derived by reworking of an altered mafic protocrust, in a range of tectonic environments.

### **Acknowledgments**

This research is partly funded by the European Research Council (Grant ERC StG 279828, project MASE to J. van Hunen). We also acknowledge funding from the CNRS/INSU (Syster project “Distribution des liquides anatectiques dans la croûte continentale : une approche multi-échelle”). AV acknowledges funding from Labex VOLTAIRE (ANR-10-LABX-100-01). CCM was supported by the European Commission and the UJM through the Campus France PRESTIGE program.

Once again, most of the plotting has been done using the R/GCDkit system (<http://gcdkit.org>; Venables and Ripley, 2002; Janoušek et al., 2006; Janoušek et al., 2015), and JFM is immensely indebted to Vojtech Janoušek for writing the software and introducing him to the beauties of R in a short course in 2011. Ben Williamson kindly supplied a copy of his PhD thesis (and the associated dataset) on the Velay granite (Williamson, 1991). JFM also wishes to acknowledge all the colleagues who introduced him to the geology of the FMC and its granites, and especially B. Barbarin, JP Couturié, JL Duthou, JM Montel and C Pin. P. Bouilhol kindly commented on the Kohistan aspects of this paper. We also thank reviewers P. Cawood and C. Hawkesworth for their helpful comments, criticisms and suggestions.

This paper is dedicated to all the colleagues who wondered why we worked in the FMC (“everything has been done there, there is nothing new to find”).

## Figure captions

Figure 1. (a) location map and (b) simplified geological map of the Eastern French Massif Central (FMC). Redrawn after 1/1 000 000 scale geological map of France (Chantraine et al., 1996), and Laurent et al. (2015). Colored symbols (with sample references) show the location of samples for which Hf isotopes in zircons were analyzed.

Figure 2. Major element properties (focussing on aluminosity) of E-FMC granitoids. (a—c) A/CNK vs. A/NK diagram (Shand, 1943) [molar Al/Ca+Na+K vs. Al/Na+K]; (b) and (c) are close-ups on the granite portion of (a). (b): MPG and CPG (including Velay and Margeride varieties); (c): KCG, Vaugnerites and microgranular mafic enclaves. (d—f): B—A diagrams (Debon and Lefort, 1983; Villaseca et al., 1998). A: molar Al-(K+Na+2Ca), B=molar Fe+Mg+Ti. (d): MPG; (e): CPG (including Margeride and Velay); (f): KCG, vaugnerites and enclaves. Larger symbols correspond to sample analyzed for Hf isotopes. The full dataset is available as Supplementary Electronic item SE1.

Figure 3. REE patterns (Nakamura, 1974) for the 4 type of granitoids described here, plus vaugnerites. Larger symbols correspond to samples analyzed for Hf isotopes. Symbols as in Fig. 2.

Figure 4.  $\epsilon_{\text{Hf}}(t)$  vs. age for all analyzed zircons in the FMC (inherited and magmatic). Symbols as in Fig. 2. Error bars on Y are  $2\sigma$ ; errors on X are typically smaller than the symbols. An evolution line for a reservoir having  $^{176}\text{Lu}/^{177}\text{Hf}$  is indicated, as well as the field of vaugnerites zircons from Couzinié et al. (2015a, 2015b) (C'16).

Figure 5. Compositions of experimental liquids ( $\text{SiO}_2 > 62\%$ ), projected from biotite onto the  $\text{Ca+Al} - 3\text{Al} + 2(\text{Na+K}) - \text{Al}+(\text{Na+K})$  plane. This figure is similar to Figure A4.6 (SE4), except that the compositions here are filtered for  $\text{SiO}_2$ . Colors correspond to the composition of the source (experimental starting material) of each glass, see SE4 for further details. This diagram is projected from  $\text{H}_2\text{O}$  (and quartz, biotite, and minor components), consequently the compositions are effectively normalized to a common total.

Figure 6. Composition of FMC granites, projected from biotite onto the  $\text{Ca+Al} - 3\text{Al} + 2(\text{Na+K}) - \text{Al}+(\text{Na+K})$  plane. Colored arrows on each panel show the main trend defined by the other types of FMC granites for reference (yellow: MPG, red: CPG, orange: Velay, Purple: KCG). The dashed purple line in (c) (“Vgn.”) illustrates the evolution of vaugnerites, although this projection is not suited for such mafic compositions.

Figure 7. Compilation of Sr-Nd isotopic data for various rocks of the FMC. All initial values are recalculated at 315 Ma, corresponding to the average emplacement age of the granitoids. For many samples, either Sr or Nd isotopes are available, but not both; therefore the data is plotted in  $\epsilon_{\text{Nd}}(t)$  vs.  $87\text{Sr}/86\text{Sr}_i$  diagram (a, middle) when data for both system are available; or in Sr vs.  $87\text{Sr}/86\text{Sr}_i$  (b) and



in  $\epsilon_{Nd}(t)$  vs. Nd (c) when only one isotopic system was analysed. The full dataset is available as supplementary item SE5. Symbols for Eastern FMC granites (and vaugnerites) are same as Fig. 2; for Limousin (Western FMC) they are smaller and duller. Brown and green field correspond to the range of isotopic compositions (at 315 Ma) of ortho and paragneisses, including both Eastern and Western FMC samples. Thick grey lines correspond to CHUR values. The whole database is available as Supplementary Electronic item SE5.

Figure 8. Potential sources of FMC granitoids, compared to experimental sources yielding liquids of contrasting compositions (cf. Fig. 5 and SE4). The light colored background fields show the range of experimental starting materials; the “pink” experimental sources produce liquids similar to KCG, the green sources yield liquids comparable to MPG and the orange sources form liquids close to CPG. The dots correspond to actual FMC rocks that are potential sources for the granites. Blue triangles are vaugnerites, associated with KCG and whose composition is similar to the material required as a source for KCG. Brown circles and diamonds correspond to orthogneisses and leucogneisses (“Leptynites”, locally; Barbey et al., 2015), similar to the required CPG source. Green crosses correspond to paragneisses or their low-grade equivalents (Cévennes schists), that resemble the source able to form MPG. (a) Total alkali vs. silica (TAS) diagram of Le Bas et al. (1986); (b) CaO vs.  $Al_2O_3$ ; (c) MFW diagram of Ohta and Arai (2007). This diagram is designed to show the effects of differentiation and alteration on mafic rocks, by combining several indicators. M corresponds to mafic rocks, F to felsic rocks and W to weathered compositions:

$$M = -0.395 \times \ln(SiO_2) + 0.206 \times \ln(TiO_2) - 0.316 \times \ln(Al_2O_3) + 0.160 \times \ln(Fe_2O_3) + 0.246 \times \ln(MgO) + 0.368 \times \ln(CaO^*) + 0.073 \times \ln(Na_2O) - 0.342 \times \ln(K_2O) + 2.266$$

$$F = 0.191 \times \ln(SiO_2) - 0.397 \times \ln(TiO_2) + 0.020 \times \ln(Al_2O_3) - 0.375 \times \ln(Fe_2O_3) - 0.243 \times \ln(MgO) + 0.079 \times \ln(CaO^*) + 0.392 \times \ln(Na_2O) + 0.333 \times \ln(K_2O) - 0.892$$

$$W = 0.203 \times \ln(SiO_2) + 0.191 \times \ln(TiO_2) + 0.296 \times \ln(Al_2O_3) + 0.215 \times \ln(Fe_2O_3) - 0.002 \times \ln(MgO) - 0.448 \times \ln(CaO^*) - 0.464 \times \ln(Na_2O) + 0.008 \times \ln(K_2O) - 1.374$$

Where  $CaO^*$  denotes CaO corrected for apatite and carbonates.

Figure 9. Location map (a, redrawn from Bouilhol et al., 2013) and geological map (b, redrawn from Jagoutz et al., 2011) of the Kohistan arc. The FMC (c) and the whole Variscan belt (d) are shown at the same scale for comparison purpose (for caption of panel c, see Figure 1, also note that this map has been simplified).

Figure 10. Major elements geochemistry of the Kohistan batholith (Dhuime et al., 2009; Jagoutz et al., 2009; Jagoutz, 2010; Bouilhol et al., 2011), compared to FMC granitoids (colored fields/arrows, same color code as Fig. 2 and Fig. 6, except in panel (a) where the pink field encompasses all FMC

granites). (a) A/CNK vs. A/NK diagram (Shand, 1943) [molar Al/Ca+Na+K vs. Al/Na+K]; (b): B—A diagrams (Debon and Lefort, 1983; Villaseca et al., 1998). A: molar Al-(K+Na+2Ca), B=molar Fe+Mg+Ti; (c) projection from biotite onto the Ca+Al – 3Al + 2(Na+K) – Al+(Na+K) plane; (d) SiO<sub>2</sub> vs. mg# [molar Mg/(Mg+Fe)x100].

Figure 11. Ree patterns (Nakamura, 1974) for the Kohistan batholith. Same dataset as fig. 10. Fields in background correspond to FMC granitoids.

Figure 12. Zircon U—Pb (left, a—c),  $\epsilon_{\text{Hf}}(t)$  (middle, d—f) and T vs.  $\epsilon_{\text{Hf}}(t)$  (right, g—i) patterns for FMC and Kohistan granitoids. (a), (d) and (g): FMC “crustal” granitoids (CPG including Velay and MPG) (Couzinié et al., 2014; Laurent et al. 2015); (b), (e) and (h): FMC KCG (Couzinié et al., 2014; Laurent et al. 2015); (c), (f) and (i): Kohistan batholith (Bosch et al., 2011; Bouilhol et al., 2013). For U—Pb age histograms, only spots > 90% concordant were considered. For Hf, only magmatic zircons were kept. In diagrams a—f, both the histograms (bars) and the probability density function (pdf, curves) are shown; pdf were calculated using a kernel density estimate as implemented in R (Venables and Ripley, 2002), i.e. with a gaussian kernel and a bandwidth defined using the method in Silverman (1986). Grey bars in (d—f) correspond to the CHUR and the depleted mantle (DM) at the relevant age (Griffin et al., 2000). The same DM evolution model appears in (g—i). Note that the time scales in (a—c) and (g—i) are offset so that the emplacement ages are aligned.

Figure 13. End-member scenarios for granite genesis at convergent plate boundaries. (a) Convergent plate boundaries can be classified according to two criteria (Vanderhaeghe and Duchene, 2010), the coupling (or decoupling) between the crust and the mantle and the advancing or retreating nature of the system. Coupled systems (A and C) can include either oceanic (blue, A1 & C1) or continental (pink, A2 & C2) crust. Decoupled systems (B and D) are depicted only with continental crust. (b) Evolution of a subduction—collision—collapse orogeny in this system. Early subduction enriches the mantle (blue star) and favors future mantle melting during late collapse/delamination. Early thickening favors future melting during the collapse stage (yellow star). (c) Evolution of a continental arc with alternating phases of slab advance and retreat. The mantle flux remains high, but slab advance periods result in crustal thickening (yellow star) and mantle enrichment (blue), that will promote melting from these two sources during retreat phases.

Figure 14. Major elements geochemistry of an example of TTG suite (the ca. 3.45 Ga Stolzberg pluton, Barberton granite-greenstone terrain of South Africa: Moyen et al., 2007), using the same diagrams as Fig. 10. The colored arrows/fields represent the composition of FMC (colors as in Fig. 2) or Kohistan (blue) granitoids.

## References

- Adam, J., Rushmer, T., O'Neil, J. and Francis, D., 2012. Hadean greenstones from the Nuvvuagittuq fold belt and the origin of the Earth's early continental crust. *Geology*, 40(4): 363-366.
- Annen, C., Blundy, J. and Sparks, R., 2006. The genesis of intermediate and silicic magmas in deep crustal hot zones. *Journal of Petrology*, 47(3): 505-539.
- Arenas, R. et al., 2007. Paleozoic ophiolites in the Variscan suture of Galicia (northwest Spain): distribution, characteristics, and meaning. *Geological Society of America Memoirs*, 200: 425-444.
- Arndt, N.T., 2013. The formation and evolution of the continental crust. *Geochemical Perspectives*, 2(3): 405-405.
- Averbuch, O. and Piromallo, C., 2012. Is there a remnant Variscan subducted slab in the mantle beneath the Paris basin? Implications for the late Variscan lithospheric delamination process and the Paris basin formation. *Tectonophysics*, 558-559: 70-83.
- Ballèvre, M. et al., 2014. Correlation of the nappe stack in the Ibero-Armorican arc across the Bay of Biscay: a joint French–Spanish project. *Geological Society, London, Special Publications*, 405(1): 77-113.
- Barbarin, B., 1999. A review of the relationships between granitoid types, their origins and their geodynamic environments. *Lithos*, 46(3): 605-626.
- Barbey, P. et al., 1999. Cordierite growth textures and the conditions of genesis and emplacement of crustal granitic magmas: the Velay granite complex (Massif Central, France). *Journal of Petrology*, 40(9): 1425-1441.
- Barbey, P., Villaros, A., Marignac, C. and Montel, J.M., 2015. Multiphase melting, magma emplacement and P-T-time path in late-collisional context: the Velay example (Massif Central, France). *Bulletin De La Societe Geologique De France*, 186(2-3): 93-116.
- Bea, F., 2012. The sources of energy for crustal melting and the geochemistry of heat-producing elements. *Lithos*, 153: 278-291.
- Becq-Giraudon, J.F., Montenat, C. and Van Den Driessche, J., 1996. Hercynian high-altitude phenomena in the French Massif Central: tectonic implications. *Palaeogeography, Palaeoclimatology, Palaeoecology*, 122(1-4): 227-241.
- Bédard, J., 2006. A catalytic delamination-driven model for coupled genesis of Archaean crust and sub-continental lithospheric mantle. *Geochimica et Cosmochimica Acta*, 70: 1188-1214.
- Bédard, J., Harris, L. and Thurston, P., 2012. The hunting of the snArc. *Precambrian Research*.
- Belousova, E. et al., 2010. The growth of the continental crust: constraints from zircon Hf-isotope data. *Lithos*, 119(3): 457-466.
- Berger, J. et al., 2010. New occurrence of UHP eclogites in Limousin (French Massif Central): Age, tectonic setting and fluid-rock interactions. *Lithos* 118:365-382.
- Bernard-Griffiths, J. and Jahn, B.-M., 1981. REE geochemistry of eclogites and associated rocks from Sauviat-sur-Vige, Massif Central, France. *Lithos*, 14: 263-274.
- Block, S., Jessell, M., Ailleres, L., Baratoux, L., Bruguier, O., Zeh, A., Bosch, D., Caby, R., Mensah, E. Lower crust exhumation during Paleoproterozoic (Eburnean) orogeny, NW Ghana, West African Craton: Interplay of coeval contractional deformation and extensional gravitational collapse. *Precambrian Research* 274:82-109
- Bonin, B., 1990. From orogenic to anorogenic settings: evolution of granitoid suites after a major orogenesis. *Geological Journal*, 25(3-4): 261-270.
- Bonin, B., 2004. Do coeval mafic and felsic magmas in post-collisional to within-plate regimes necessarily imply two contrasting, mantle and crustal, sources? A review. *Lithos*, 78(1-24).
- Bosch, D. et al., 2011. Building an island-arc crustal section: Time constraints from a LA-ICP-MS zircon study. *Earth and Planetary Science Letters*, 309: 268-279.
- Bosse V., Feraud G., Ruffet G., Balleve M., Peucat JJ., De Jong K., 2000. Late Devonian subduction and early –orogenic exhumation of eclogite-facies rocks from the Champtoceaux Complex (Variscan belt, France). *Geological Journal*, 34(3-4): 297-325.
- Bouilhol, P. et al., 2011. Timing of juvenile arc crust formation and evolution in the Sapat Complex (Kohistan–Pakistan). *Chemical Geology*, 280(3): 243-256.

- Bouilhol, P., Jagoutz, O., Hanchar, J.M. and Dudas, F.O., 2013. Dating the India–Eurasia collision through arc magmatic records. *Earth and Planetary Science Letters*, 366: 163-175.
- Bouvier, A., Vervoort, J.D. and Patchett, P.J., 2008. The Lu-Hf and Sm-Nd isotopic composition of CHUR: Constraints from unequilibrated chondrites and implications for the bulk composition of terrestrial planets. *Earth and Planetary Science Letters*, 273: 48-57.
- Burg, J.-P. and Vanderhaeghe, O., 1993. Structures and way-up criteria in migmatites, with application to the Velay dome (French Massif Central). *Journal of structural geology*, 15(11): 1293-1301.
- Burg, J. and Matte, P., 1978. A cross section through the French Massif Central and the scope of its Variscan geodynamic evolution. *Zeitschrift der Deutschen Geologischen Gesellschaft*, 129: 429-460.
- Burg, J., Matte, P., Leyreloup, A. and Marchand, J., 1984. Inverted metamorphic zonation and large-scale thrusting in the Variscan Belt: an example in the French Massif Central. *Geological Society, London, Special Publications*, 14(1): 47-61.
- Cawood, P.A. et al., 2009. Accretionary orogens through Earth history. *Geological Society, London, Special Publications*, 318(1): 1-36.
- Cawood, P.A., Hawkesworth, C. and Dhuime, B., 2013. The continental record and the generation of continental crust. *Geological Society of America Bulletin*, 125(1-2): 14-32.
- Chantraine, J., Autran, A. and Cavalier, C., 1996. Carte géologique de la France à l'échelle du millionième (6e édition), BRGM, Orléans.
- Chappell, B.W. and White, A.J.R., 1974. Two contrasting granite types. *Pacific Geology*, 8: 173-174.
- Chappell, B.W., White, A.J.R. and Wyborn, D., 1987. The Importance of Residual Source Material (Restite) in Granite Petrogenesis. *Journal of Petrology*, 28(6): 1111-1138.
- Chappell, B.W., White, A.J.R., Williams, I.S., Wyborn, D. and Wyborn, L.A.I., 2000. Lachlan Fold Belt granites revisited: High- and low-temperature granites and their implications. *Australian Journal of Earth Sciences*, 47: 123-138.
- Chardon, D., Gapais, D. and Cagnard, F., 2009. Flow of ultra-hot orogens: A view from the Precambrian, clues for the Phanerozoic. *Tectonophysics*, 477(3-4): 105-118.
- Chelle-Michou, C., Laurent, O., Moyen, J.F., Block, S., Gardien, V., Paquette, J.L., Couzinié, S., 2015. New U-Pb and Hf zircon data from the eastern Massif Central: From Gondwana to Pangea in a nutshell, Variscan conference, Rennes, June 2015.
- Clarke, D.B., Paterson, S.R. and Vernon, R.H., 2007. Contaminated granites: preface. *The Canadian Mineralogist*, 45(1): 1-3.
- Clemens, J.D. and Watkins, J.M., 2001. The fluid regime of high-temperature metamorphism during granitoid magma genesis. *Contribution to Mineralogy and Petrology*, 140: 600-606.
- Clemens, J.D., 2003. S-type granitic magmas - petrogenetic issues, models and evidence. *Earth-Science Reviews*, 61(1-2): 1-18.
- Clift, P. and Vannucchi, P., 2004. Controls on tectonic accretion versus erosion in subduction zones: Implications for the origin and recycling of the continental crust. *Reviews of Geophysics*, 42(2).
- Clift, P.D., Vannucchi, P. and Morgan, J.P., 2009. Crustal redistribution, crust–mantle recycling and Phanerozoic evolution of the continental crust. *Earth-Science Reviews*, 97(1): 80-104.
- Collins, W.J., 2002. Hot orogens, tectonic switching, and creation of continental crust. *Geology*, 30(6): 535-538.
- Conceicao, R.V. and Green, D.H., 2004. Derivation of potassic (shoshonitic) magmas by decompression melting of phlogopite plus pargasite lherzolite. *Lithos*, 72(3-4): 209-229.
- Condamine, P. and Médard, E., 2014. Experimental melting of phlogopite-bearing mantle at 1 GPa: implications for potassic magmatism. *Earth and Planetary Science Letters*, 397: 80-92.
- Condie, K.C., Bickford, M., Aster, R.C., Belousova, E. and Scholl, D.W., 2011. Episodic zircon ages, Hf isotopic composition, and the preservation rate of continental crust. *Geological Society of America Bulletin*, 123(5-6): 951-957.
- Couzinié, S. et al., 2014. Temporal relationships between Mg-K mafic magmatism and catastrophic melting of the Variscan crust in the southern part of the Velay Complex (Massif Central, France). *Journal of Geosciences*, 59(1-4): 1-18.

- Couzinié, S., Laurent, O., Moyen, J.F., Zeh, A., Vézinet, A., Villaros, A., Gardien, V., 2015a. Mg-K magmatic suites as a tool to scan the composition of the Variscan orogenic mantle, case studies from the French Massif Central, Variscan conference, Rennes.
- Couzinié, S., Laurent, O., Moyen, J.F., Zeh, A., Villaros, A., Bouilhol, P., 2015b. Lithospheric mantle melting during continental collision: crustal growth or crustal recycling? A case study from the Variscan French Massif Central, Eighth Hutton symposium on granites and related rocks, Florianopolis, Brazil.
- Crawford, M.B. and Searle, M.P., 1992. Field Relationships and Geochemistry of Pre-Collisional (India-Asia) Granitoid Magmatism in the Central Karakoram, Northern Pakistan. *Tectonophysics*, 206(1-2): 171-192.
- Dall'Agnol, R. and de Oliveira, D.C., 2007. Oxidized, magnetite-series, rapakivi-type granites of Carajás, Brazil: implications for classification and petrogenesis of A-type granites. *Lithos*, 93(3): 215-233.
- Davidson, J., Turner, S., Handley, H., Macpherson, C. and Dosseto, A., 2007. Amphibole "sponge" in arc crust? *Geology*, 35(9): 787-790.
- Debon, F., LeFort, P., Sheppard, S.M.F. and Sonnet, J. 1986. The four plutonic belts of the Trans-Himalaya: A chemical, mineralogical, isotopic and chronological synthesis along the Tibet-Nepal Section. *Jour. Petr.*, 27: 219-250.
- Debon, F. and Lefort, P., 1983. A chemical–mineralogical classification of common plutonic rocks and associations. *Transactions of the Royal Society of Edinburgh: Earth Sciences*, 73(135-149).
- Debon, F., Le Fort, P., Dautel, D., Sonet, J. and Zimmermann, J., 1987. Granites of western Karakorum and northern Kohistan (Pakistan): a composite Mid-Cretaceous to upper Cenozoic magmatism. *Lithos*, 20(1): 19-40.
- Debon, F., Lemmet, M., 1999. Evolution of Fe/Mg ratios in Late Variscan plutonic rocks from the External Crystalline Massif of the Alps (France, Italy, Switzerland). *Journal of Petrology* 40 (7), 1151–1185.
- DeCelles, P.G., Ducea, M.N., Kapp, P. and Zandt, G., 2009. Cyclicity in Cordilleran orogenic systems. *Nature Geoscience*, 2(4): 251-257.
- Depine, G.V., Andronicos, C.L. and Phipps-Morgan, J., 2008. Near-isothermal conditions in the middle and lower crust induced by melt migration. *Nature*, 452(7183): 80-83.
- de Sigoyer J., Vanderhaeghe O., Duchêne S., Billerot A., 2014. Generation and emplacement of Triassic granitoids within the Songpan Ganze accretionary-orogenic wedge in a context of slab retreat accommodated by tear faulting, Eastern Tibetan plateau, China. *Journal of Asian Earth Sciences*, 88, 192-216.
- Dhuime, B. et al., 2009. Geochemical architecture of the lower-to middle-crustal section of a paleo-island arc (Kohistan Complex, Jijal–Kamila area, northern Pakistan): implications for the evolution of an oceanic subduction zone. *Journal of Petrology*: egp010.
- Dhuime, B., Hawkesworth, C. and Cawood, P., 2011. When continents formed. *Science*, 331: 154-155.
- Didier, J. and Barbarin, B., 1991. *Enclaves and Granite Petrology*. Elsevier, Amsterdam.
- Didier, A. et al., 2013. Disturbance versus preservation of U–Th–Pb ages in monazite during fluid–rock interaction: textural, chemical and isotopic in situ study in microgranites (Velay Dome, France). *Contributions to Mineralogy and Petrology*: 1-22.
- Dupraz, J. and Didier, J., 1988. Le complexe anatectique du Velay (Massif Central français): structure d'ensemble et évolution géologique. *Bulletin du BRGM, v. Série "Géologie de la France" : .* 73-88.
- Duthou, J.L., Cantagrel, J.M., Didier, J. and Vialette, Y., 1984. Paleozoic Granitoids from the French Massif Central - Age and Origin Studied by Rb-87-Sr-87 System. *Physics of the Earth and Planetary Interiors*, 35(1-3): 131-144.
- Eguiluz, L., Ibarguchi, J.G., Abalos, B. and Apraiz, A., 2000. Superposed Hercynian and Cadomian orogenic cycles in the Ossa-Morena zone and related areas of the Iberian Massif. *Geological Society of America Bulletin*, 112(9): 1398-1413.

- England, P.C. and Thompson, A.B., 1984. Pressure-temperature-time paths of regional metamorphism, part I: heat transfer during the evolution of regions of thickened continental crust. *Journal of Petrology*, 25: 894-928.
- Faure, M., Lardeaux, J.M. and Ledru, P., 2009a. A review of the pre-Permian geology of the Variscan French Massif Central. *Comptes Rendus Geosciences*, 341(2-3): 202-213.
- Faure, M., Mezeme, E.B., Cocherie, A., Melleton, J. and Rossi, P., 2009b. The South Millevalches Middle Carboniferous crustal melting and its place in the French Variscan belt. *Bulletin De La Societe Geologique De France*, 180(6): 473.
- Fernández-Suárez, J. et al., 2011. Iberian late-Variscan granitoids: Some considerations on crustal sources and the significance of “mantle extraction ages”. *Lithos*, 123: 121-132.
- Finger, F., Roberts, M.P., Haunschmid, B., Schermaier, A. and Steyrer, H.P., 1997. Variscan granitoids of central Europe: their typology, potential sources and tectonothermal relations. *Mineralogy and Petrology*, 61(1-4): 67-96.
- Fowler, M., Kocks, H., Darbyshire, D. and Greenwood, P., 2008. Petrogenesis of high Ba–Sr plutons from the Northern Highlands Terrane of the British Caledonian Province. *Lithos*, 105(1): 129-148.
- Fowler, M.B., 1988. Achuaine Hybrid Appinite Pipes - Evidence for Mantle-Derived Shoshonitic Parent Magmas in Caledonian Granite Genesis. *Geology*, 16(11): 1026-1030.
- Fowler, M., Henney, P.J., 1996. Mixed Caledonian appinite magmas: implications for lamprophyre fractionation and high Ba-Sr granite genesis. *Contributions to Mineralogy and Petrology* 126, 199-215.
- Frost, B.R. et al., 2001. A geochemical classification for granitic rocks. *Journal of Petrology*, 42(11): 2033-2048.
- Gardien, V., Tegye, M., Lardeaux, J.-M., Misseri, M. and Dufour, E., 1990. Crust–mantle relationships in the French Variscan chain: the examples of the southern Monts du Lyonnais unit (eastern French Massif Central). *Journal of Metamorphic Geology*, 8: 447-492.
- Gardien, V., Thompson, A.B., Grujic, D. and Ulmer, P., 1995. Experimental melting of biotite + plagioclase + quartz + or - muscovite assemblages and implications for crustal melting. *Journal of Geophysical Research, B, Solid Earth and Planets*, 100(8): 15,581-15,591.
- Gardien, V., Lardeaux, J.-M., Ledru, P., Allemand, P. and Guillot, S., 1997. Metamorphism during late orogenic extension: insights from the French Variscan belt. *Bulletin de la Société Géologique de France*, 168(3): 271-286.
- Gébelin, A., Roger, F. and Brunel, M., 2009. Syntectonic crustal melting and high-grade metamorphism in a transpressional regime, Variscan Massif Central, France. *Tectonophysics*, 477(3-4): 229-243.
- Gerdes, A. and Zeh, A., 2006. Combined U–Pb and Hf isotope LA-(MC-)ICP-MS analyses of detrital zircons: Comparison with SHRIMP and new constraints for the provenance and age of an Armorican metasediment in Central Germany. *Earth and Planetary Science Letters*, 249(1-2): 47-61.
- Gerdes, A. and Zeh, A., 2009. Zircon formation versus zircon alteration—new insights from combined U–Pb and Lu–Hf in-situ LA-ICP-MS analyses, and consequences for the interpretation of Archean zircon from the Central Zone of the Limpopo Belt. *Chemical Geology*, 261(3): 230-243.
- Griffin, W. et al., 2000. The Hf isotope composition of cratonic mantle: LAM-MC-ICPMS analysis of zircon megacrysts in kimberlites. *Geochimica et Cosmochimica Acta*, 64(1): 133-147.
- Griffin, W. et al., 2002. Zircon chemistry and magma mixing, SE China: in-situ analysis of Hf isotopes, Tonglu and Pingtan igneous complexes. *Lithos*, 61(3): 237-269.
- Guitreau, M., Blichert-Toft, J., Martin, H., Mojzsis, S.J. and Albarède, F., 2012. Hafnium isotope evidence from Archean granitic rocks for deep-mantle origin of continental crust. *Earth and Planetary Science Letters*, 337-338: 211-223.
- Hamilton, W.B., 1998. Archean magmatism and deformation were not products of plate tectonics. *Precambrian Research*, 91(1-2): 143-179.
- Hamilton, W.B., 2003. An alternative earth. *GSA Today*, 13(11): 4-12.
- Hawkesworth, C., Cawood, P., Kemp, T., Storey, C. and Dhuime, B., 2009. Geochemistry: A matter of preservation. *Science*, 323: 49-50.

- Hawkesworth, C. et al., 2010. The generation and evolution of the continental crust. *Journal of the Geological Society*, 167(2): 229-248.
- Heilimo, E., Halla, J. and Hölttä, P., 2010. Discrimination and origin of the sanukitoid series: Geochemical constraints from the Neoproterozoic western Karelian Province (Finland). *Lithos*, 115(1-4): 27-39.
- Hildreth, W. and Moorbath, S., 1988. Crustal contributions to arc magmatism in the Andes of central Chile. *Contributions to mineralogy and petrology*, 98(4): 455-489.
- Holliger, P., Cuney, M., Friedrich, M. and Turpin, L., 1986. Age carbonifère de l'unité de Brame du complexe granitique peralumineux de Saint-Sylvestre (NO Massif Central) défini par les données isotopiques U-Pb sur zircon et monazite. *Comptes rendus de l'Académie des sciences. Série 2, Mécanique, Physique, Chimie, Sciences de l'univers, Sciences de la Terre*, 303(14): 1309-1314.
- Holub, F.V., 1997. Ultrapotassic plutonic rocks of the durbachite series in the Bohemian Massif: petrology, geochemistry and petrogenetic interpretation. *Sborník geologických věd, Ložisková geologie–mineralogie*, 31: 5-26.
- Ilbeyli, N., Pearce, J.A., Thirlwall, M. and Mitchell, J., 2004. Petrogenesis of collision-related plutonics in Central Anatolia, Turkey. *Lithos*, 72(3): 163-182.
- Inger, S. and Harris, N.B.W., 1993. Geochemical constraints on leucogranite magmatism in the Langtang valley, Nepal Himalayas. *Journal of Petrology*, 34(2): 345-368.
- Isozaki, Y., Aoki, K., Nakama, T. and Yanai, S., 2010. New insight into a subduction-related orogen: A reappraisal of the geotectonic framework and evolution of the Japanese Islands. *Gondwana Research*, 18(1): 82-105.
- Jagoutz, O., Müntener, O., Schmidt, M.W. and Burg, J.-P., 2011. The roles of flux- and decompression melting and their respective fractionation lines for continental crust formation: Evidence from the Kohistan arc. *Earth and Planetary Science Letters*, 303(1): 25-36.
- Jagoutz, O.E. et al., 2009. Construction of the granitoid crust of an island arc part I: geochronological and geochemical constraints from the plutonic Kohistan (NW Pakistan). *Contributions to Mineralogy and Petrology*, 158(6): 739-755.
- Jagoutz, O.E., 2010. Construction of the granitoid crust of an island arc. Part II: a quantitative petrogenetic model. *Contributions to Mineralogy and Petrology*, 160(3): 359-381.
- Janoušek, V., Holub, F.V., Rogers, G. and Bowes, D., 1997. Two distinct mantle sources of Hercynian magmas intruding the Moldanubian unit, Bohemian Massif, Czech Republic. *Journal of GEOsciences*, 42(3): 10-0.
- Janoušek, V., Bowes, D., Rogers, G., Farrow, C.M. and Jelínek, E., 2000. Modelling diverse processes in the petrogenesis of a composite batholith: the Central Bohemian Pluton, Central European Hercynides. *Journal of Petrology*, 41(4): 511.
- Janoušek, V., Farrow, G. and Erban, V., 2006. Interpretation of Whole-rock Geochemical Data in Igneous Geochemistry: Introducing Geochemical Data Toolkit (GCDkit). *Journal of Petrology*, 47(6): 1255-1259.
- Janoušek, V., Holub, F.V., Magna, T. and Erban, V., 2010. Isotopic constraints on the petrogenesis of the Variscan ultrapotassic magmas from the Moldanubian Zone of the Bohemian Massif. *Mineralogia: Special papers*, 37: 32-36.
- Janoušek, V., Moyen, J.F., Martin, H., Erban, V. and Farrow, C.M., 2015. *Geochemical Modelling of Igneous Processes—Principles and Recipes in the R Language*. Springer Verlag, Berlin.
- Kamber, B., Ewart, A., Collerson, K.D., Bruce, M.C. and McDonald, G.D., 2002. Fluid-mobile trace elements constraints on the role of slab melting and implications for Archaean crustal growth models. *Contributions to Mineralogy and Petrology*, 144: 38-56.
- Kemp, A.I., Hawkesworth, C.J., Paterson, B.A., Kinny, P.D., 2006. Episodic growth of the Gondwana supercontinent from hafnium and oxygen isotopes in zircon. *Nature* 439, 580-583.
- Kemp, A., Hawkesworth, C., Collins, W., Gray, C. and Blevin, P., 2009. Isotopic evidence for rapid continental growth in an extensional accretionary orogen: The Tasmanides, eastern Australia. *Earth and Planetary Science Letters*, 284(3): 455-466.
- Kleinhans, I.C., Kramers, J.D. and Kamber, B.S., 2003. Importance of water for Archaean granitoid petrology: a comparative study of TTG and potassic granitoids from Barberton Mountain Land, South Africa. *Contributions to Mineralogy and Petrology*, 145: 377-389.

- Kotková, J., O'Brien, P.J. and Ziemann, M.A., 2011. Diamond and coesite discovered in Saxony-type granulite: solution to the Variscan garnet peridotite enigma. *Geology*, 39: 667-670.
- Kruckenberg S.C., Vanderhaeghe O., Ferré E.C., Teyssier C., Whitney D.L., Chapman A. (2011): Flow of partially molten crust and the internal dynamics of a migmatite dome, Naxos, Greece. *Tectonics* 30, TC3001.
- Labrousse, L., Prouteau, G. and Ganzhorn, A.-C., 2011. Continental exhumation triggered by partial melting at ultrahigh pressure. *Geology*, 39(12): 1171-1174.
- Lagarde, J.-L., Dallain, C., Ledru, P. and Courrioux, G., 1994. Strain patterns within the late Variscan granitic dome of Velay, French Massif Central. *Journal of Structural Geology*, 16(6): 839-852.
- Lardeaux, J.M. et al., 2014. The Moldanubian Zone in the French Massif Central, Vosges/Schwarzwald and Bohemian Massif revisited: differences and similarities. In: K. Schulmann, J.R. Martinez Catalan, J.M. Lardeaux, V. Janousek and G. Oggiano (Editors), *The Variscan Orogeny: Extent, Timescale and the Formation of the European Crust*. Special publications. Geological Society, London.
- Lasnier, B., 1971. Les péridotites et pyroxénolites à grenat du Bois des feuilles (Monts du lyonnais) (France). *Contributions to Mineralogy and Petrology*, 34(1): 29-42.
- Laurent, O., Doucelance, R., Martin, H. and Moyen, J.-F., 2012. Differentiation of the late-Archaean sanukitoid series and some implications for crustal growth: insights from geochemical modelling on the Bulai pluton, Central Limpopo Belt, South Africa. *Precambrian Research*, 227: 188-203.
- Laurent, O., Martin, H., Moyen, J.-F. and Doucelance, R., 2014a. The diversity and evolution of late-Archaean granitoids: evidence for the onset of "modern-style" plate tectonics between 3.0 and 2.5 Ga. *Lithos*, 205: 208-235.
- Laurent, O. et al., 2014b. Contrasting petrogenesis of Mg-K and Fe-K granitoids and implications for postcollisional magmatism: case study from the late-Archaean Matok pluton (Pietersburg block, South Africa). *Lithos*, 196-197: 131-149.
- Laurent, O. and Zeh, A., 2015. A linear Hf isotope-age array despite different granitoid sources and complex Archean geodynamics: Example from the Pietersburg block (South Africa). *Earth and Planetary Science Letters*, 430: 326-338.
- Laurent, O., Couzinié, S., Vanderhaeghe, O., Zeh, A., Moyen, J.F., Villaros, A., Gardien, V., 2015. U–Pb dating of Variscan igneous rocks from the eastern French Massif Central: southward migration of coeval crust- and mantle- melting witnesses late-orogenic slab retreat, Variscan conference, Rennes, June 2015.
- Le Bas, M.J., Le Maître, R.W., Streckeisen, A. and Zanettin, B., 1986. A chemical classification of volcanic rocks based on the total alkali-silica diagram. *Journal of Petrology*, 27: 745-750.
- Ledru, P. et al., 1989. Où sont les Nappes dans le Massif Central Français? *Bulletin De La Societe Geologique De France*, 5(3): 605-618.
- Ledru, P. et al., 2001. The Velay dome (French Massif Central): melt generation and granite emplacement during orogenic evolution. *Tectonophysics*, 342(3-4): 207-237.
- Linnemann, U., Gerdes, A., Hofmann, M. and Marko, L., 2013. The Cadomian Orogen: Neoproterozoic to Early Cambrian crustal growth and orogenic zoning along the periphery of the West African Craton—Constraints from U–Pb zircon ages and Hf isotopes (Schwarzburg Antiform, Germany). *Precambrian Research*, 244: 236-278.
- Malavieille, J., Guihot, P., Costa, S., Lardeaux, J.M. and Gardien, V., 1990. Collapse of the thickened Variscan crust in the French Massif Central: Mont Pilat extensional shear zone and St. Etienne Late Carboniferous basin. *Tectonophysics*, 177(1-3): 139-149.
- Marschall, H.R. and Schumacher, J.C., 2012. Arc magmas sourced from mélange diapirs in subduction zones. *Nature Geoscience*, 5: 862-867.
- Martin, H., 1986. Effect of steeper Archean geothermal gradient on geochemistry of subduction-zone magmas. *Geology*, 14(9): 753-756.
- Martin, H., 1994. The Archean grey gneisses and the genesis of the continental crust. In: K.C. Condie (Editor), *Archean crustal evolution*. *Developments in Precambrian Geology*. Elsevier, Amsterdam, pp. 205-259.
- Martin, H., Moyen, J.-F. and Rapp, R., 2010. Sanukitoids and the Archean-Proterozoic boundary. *Transactions of the Royal Society of Edinburgh-Earth Sciences*, 100(1-2): 15-33.



- Martin, H., Moyen, J.-F., Guitreau, M., Blichert-Toft, J. and Le Pennec, J.-L., 2014. Why archaean TTG cannot be generated by MORB melting in subduction zone. *Lithos*, 198-199: 1-13.
- Matte, P., 1986. Tectonics and Plate-Tectonics Model for the Variscan Belt of Europe. *Tectonophysics*, 126(2-4): 329-374.
- Melleton, J., Cocherie, A., Faure, M. and Rossi, P., 2010. Precambrian protoliths and Early Paleozoic magmatism in the French Massif Central: U-Pb data and the North Gondwana connection in the west European Variscan belt. *Gondwana Research*, 17(1): 13-25.
- Menant A., Jolivet L., Vrielynck B. 2016. Kinematic reconstructions and magmatic evolution illuminating crustal and mantle dynamics of the eastern Mediterranean region since the late Cretaceous. *Tectonophysics* 675, 103–140.
- Merle, O. and Michon, L., 2001. The formation of the West European Rift; a new model as exemplified by the Massif Central area. *Bulletin De La Societe Geologique De France*, 172(2): 213-221.
- Michon, G., 1987. Les Vaugnerites de l'Est du Massif Central Français : Apport de l'Analyse Multivariée à l'Etude Géochimique des Eléments Majeurs Statistical Approach on Major Elements. *Bulletin De La Societe Geologique De France*, 3(3): 591-600.
- Miller, C.F., McDowell, S.M. and Mapes, R.W., 2003. Hot and cold granites? Implications of zircon saturation temperatures and preservation of inheritance. *Geology*, 31(6): 529-532.
- Mintrone, M., 2015. Le Massif Central avant la chaîne varisque. M1 thesis, Université Blaise-Pascal, Clermont-Ferrand.
- Montel, J.-M., 1993. A model for monazite/melt equilibrium and application to the generation of granitic magmas. *Chemical Geology*, 110(1-3): 127-146.
- Montel, J.-M. and Abdelghaffar, R., 1993. Les granites tardimigmatitiques du Velay (Massif central): principales caractéristiques pétrographiques et géochimiques. *Géologie de la France*, 1: 15-28.
- Montel, J.M., Marignac, C., Barbey, P. and Pichavant, M., 1992. Thermobarometry and Granite Genesis - the Hercynian Low-P, High-T Velay Anatectic Dome (French Massif-Central). *Journal of Metamorphic Geology*, 10(1): 1-15.
- Morag, N., Avigad, D., Gerdes, A., Belousova, E., Harlavan, Y., 2011. Crustal evolution and recycling in the northern Arabian-Nubian Shield: New perspectives from zircon Lu-Hf and U-Pb systematics. *Precambrian Res* 186, 101-116.
- Moyen, J.-F., Stevens, G., Kisters, A.F.M. and Belcher, R.W., 2007. TTG plutons of the Barberton granitoid-greenstone terrain, South Africa. In: M.J. Van Kranendonk, R.H. Smithies and V. Bennett (Editors), *Earth's Oldest rocks. Developments in Precambrian geology*. Elsevier, pp. 606--668.
- Moyen, J.-F., 2011. The composite Archaean grey gneisses: petrological significance, and evidence for a non-unique tectonic setting for Archaean crustal growth. *Lithos*, 123: 21-36.
- Moyen, J.-F. and Martin, H., 2012. Forty years of TTG research. *Lithos*, 148: 312-336.
- Moyen, J.-F. and van Hunen, J., 2012. Short term episodicity of Archaean subduction. *Geology*, 40(5): 451-454.
- Moyen, J.F., Martin, H. and Jayananda, M., 2001. Multi-element geochemical modelling of crust-mantle interactions during late-Archaean crustal growth: the Closepet granite (South India). *Precambrian Research*, 112(1-2): 87-105.
- Nagel, T.J., Hoffmann, J.E. and Münker, C., 2012. Melting of EoArchaean TTGs from thickened mafic arc crust. *Geology*, 40: 375-378.
- Nakamura, N., 1974. Determination of REE, Ba, Fe, Mg, Na and K in carbonaceous and ordinary chondrites. *Geochimica et Cosmochimica Acta*, 38: 757-775.
- Nance, D.R., Murphy, B.J., Strachan, R.A., D'Lemos, R.S. and Taylor, G.K., 1991. Late Proterozoic tectonostratigraphic evolution of the Avalonian and Cadomian terranes. *Precambrian Research*, 53: 41-78.
- Nance, R.D. and Murphy, J.B., 1994. Contrasting basement isotopic signatures and the palinspastic restoration of peripheral orogens: examples from the Neoproterozoic Avalonian-Cadomian Belt. *Geology*, 22: 617-620.
- Nandedkar, R., Ulmer, P. and Müntener, O., 2014. Fractional crystallization of primitive, hydrous arc magmas: an experimental study at 0.7 GPa. *Contributions to Mineralogy and Petrology*, 167(6): 1-27.

- O'Connor, J.T., 1965. A classification for quartz-rich igneous rocks based on feldspar ratios. U.S. Geological Survey Professional Paper, 525(B): 79-84.
- Ohta, T. and Arai, H., 2007. Statistical empirical index of chemical weathering in igneous rocks: A new tool for evaluating the degree of weathering. *Chemical Geology*, 240(3): 280-297.
- Patiño-Douce, A.E. and Harris, N., 1998. Experimental constraints on Himalayan anatexis. *Journal of Petrology*, 39(4): 689-710.
- Patiño-Douce, A.E., 1999. What do experiments tell us about the relative contributions of crust and mantle to the origin of granitic magmas? In: A. Castro, C. Fernandez and J.L. Vigneresse (Editors), *Understanding granites: integrating new and classical techniques*. Geological society of London special publications. Geological society, London, pp. 55-75.
- Pearce, J.A., Harris, N.B.W. and Tindle, A.G., 1984. Trace element discrimination diagrams for the tectonic interpretation of granitic rocks. *Journal of Petrology*, 25: 956-983.
- Pe-Piper, G., and Piper, D.J.W., 2006, Unique features of the Cenozoic igneous rocks of Greece, in Dilek, Y., and Pavlides, S., eds., *Postcollisional tectonics and magmatism in the Mediterranean region and Asia: Geological Society of America Special Paper 409*, p. 259–282.
- Pin, C. and Duthou, J.L., 1990. Sources of Hercynian Granitoids from the French Massif-Central - Inferences from Nd Isotopes and Consequences for Crustal Evolution. *Chemical Geology*, 83(3-4): 281-296.
- Ploquin, A. et al., 1994. Igneous activity. Caledono-Hercynian magmatism in the French Massif Central, *Pre-Mesozoic Geology in France and Related Areas*. Springer, pp. 341-378.
- R'Kha Chaham, K., Couturié, J.-P., Duthou, J.-L., Fernandez, A. and Vitel, G., 1990. L'orthogneiss œillé de l'Arc de Fix: un nouveau témoin d'âge cambrien d'un magmatisme hyper alumineux dans le Massif Central français. *Comptes rendus de l'Académie des sciences. Série 2, Mécanique, Physique, Chimie, Sciences de l'univers, Sciences de la Terre*, 311(7): 845-850.
- Rapp, R., Shimizu, N., Norman, M.D. and Applegate, G.S., 1999. Reaction between slab-derived melts and peridotite in the mantle wedge : experimental constraints at 3.8 GPa. *Chemical Geology*, 160: 335-356.
- Rapp, R. et al., 2010. Continent Formation in the Archean and Chemical Evolution of the Cratonic Lithosphere: Melt–Rock Reaction Experiments at 3–4 GPa and Petrogenesis of Archean Mg-Diorites (Sanukitoids). *Journal of Petrology*, 51(6): 1237.
- Raumer, J.F., Finger, F., Veselá, P. and Stampfli, G.M., 2013. Durbachites–Vaugnerites—a geodynamic marker in the central European Variscan orogen. *Terra Nova*.
- Replumaz, A., Negrodo, A.M., Guillot, S., Van Der Beek, P. and Villaseñor, A., 2010. Crustal mass budget and recycling during the India/Asia collision. *Tectonophysics*, 492(1): 99-107.
- Ribeiro, A., Quesada, C. and Dallmeyer, R., 1990. Geodynamic evolution of the Iberian Massif, *Pre-Mesozoic Geology of Iberia*. Springer, pp. 399-409.
- Roberts, N.M. and Spencer, C.J., 2014. The zircon archive of continent formation through time. *Geological Society, London, Special Publications*, 389: SP389. 14.
- Rudnick, R.L., 1995. Making continental crust. *Nature*, 378: 571-578.
- Rudnick, R.L. and Gao, S., 2003. Composition of the Continental Crust. In: H.D. Holland and K.K. Turekian (Editors), *Treatise of Geochemistry*. Elsevier, Amsterdam, pp. 1-64.
- Sabatier, H., 1991. Vaugnerites: special lamprophyre-derived mafic enclaves in some Hercynian granites from Western and Central Europe. In: J. Didier and B. Barbarin (Editors), *Enclaves and granite petrology. Developments in petrology*, pp. 63-81.
- Santos, M.M. et al., in press. BB zircon – A new Sri Lankan reference material for U-Pb and Hf isotopic laser ablation ICP-MS analysis. *Geostandards and Geoanalytical Research*.
- Santosh, M., Maruyama, S. and Yamamoto, S., 2009. The making and breaking of supercontinents: some speculations based on superplumes, super downwelling and the role of tectosphere. *Gondwana Research*, 15(3): 324-341.
- Scarrow, J., Molina, J., Bea, F. and Montero, P., 2009. Within-plate calc-alkaline rocks: Insights from alkaline mafic magma–peraluminous crustal melt hybrid appinites of the Central Iberian Variscan continental collision. *Lithos*, 110(1): 50-64.

- Scarrow, J.H., Molina, J.F., Bea, F., Montero, P. and Vaughan, A.P.M., 2011. Lamprophyre dikes as tectonic markers of late orogenic transtension timing and kinematics: A case study from the Central Iberian Zone. *Tectonics*, 30(4): TC4007.
- Scherer, E., Münker, C. and Mezger, K., 2001. Calibration of the lutetium-hafnium clock. *Science*, 293(5530): 683-687.
- Scholl, D.W. and von Huene, R., 2007. Crustal recycling at modern subduction zones applied to the past—Issues of growth and preservation of continental basement crust, mantle geochemistry, and supercontinent reconstruction. *Geological Society of America Memoirs*, 200: 9-32.
- Scholl, D.W. and von Huene, R., 2009. Implications of estimated magmatic additions and recycling losses at the subduction zones of accretionary (non-collisional) and collisional (suturing) orogens. *Geological Society, London, Special Publications*, 318(1): 105-125.
- Schulmann, K., Lexa, O., Janoušek, V., Lardeaux, J.M. and Edel, J.B., 2014. Anatomy of a diffuse cryptic suture zone: An example from the Bohemian Massif, European Variscides. *Geology*, 42(4): 275-278.
- Searle, M., Cottle, J., Streule, M. and Waters, D., 2010. Crustal melt granites and migmatites along the Himalaya: melt source, segregation, transport and granite emplacement mechanisms. *Geological Society of America Special Papers*, 472: 219-233.
- Searle, M.P. et al., 1997. Shisha Pangma leucogranite, south Tibetan Himalaya: Field relations, geochemistry, age, origin, and emplacement. *Journal of Geology*, 105(3): 295-317.
- Shand, S.J., 1943. *Eruptive Rocks. Their Genesis, Composition, Classification, and Their Relation to Ore-Deposits with a Chapter on Meteorite*. John Wiley & Sons, New-York.
- Shaw, D.M., 2006. *Trace elements in magmas: a theoretical treatment*. Cambridge University Press, Cambridge, 243 pp.
- Siebel, W. and Chen, F., 2009. Zircon Hf isotope perspective on the origin of granitic rocks from eastern Bavaria, SW Bohemian Massif. *International Journal of Earth Sciences*, 99(5): 993-105.
- Silverman, B.W., 1986. *Density estimation*. Chapman and Hall, London.
- Sizova, E., Gerya, T., Brown, M. and Perchuk, L.L., 2010. Subduction styles in the Precambrian: Insight from numerical experiments. *Lithos*, 116(3-4): 209-229.
- Sizova, E., Gerya, T. and Brown, M., 2014. Contrasting styles of Phanerozoic and Precambrian continental collision. *Gondwana Research*, 25(2): 522-545.
- Skjerlie, K. and Patiño-Douce, A.E., 1995. Anatexis of interlayered amphibolite and pelite at 10 kbar: effect of diffusion of major components on phase relations and melt fraction. *Contribution to Mineralogy and Petrology*, 122: 62-78.
- Söderlund, U., Patchett, P.J., Vervoort, J.D. and Isachsen, C.E., 2004. The 176 Lu decay constant determined by Lu–Hf and U–Pb isotope systematics of Precambrian mafic intrusions. *Earth and Planetary Science Letters*, 219(3): 311-324.
- Solgadi, F., Moyen, J.-F., Vanderhaeghe, O., Sawyer, E.W. and Reisberg, L., 2007. The relative roles of crustal anatexis and mantle-derived magmas: Generation of Synorogenic, Hercynian granites in the Livradois area, French Massif Central. *Canadian Mineralogist*, 45: 581-606.
- Spencer, C.J. et al., 2015. Generation and preservation of continental crust in the Grenville Orogeny. *Geoscience Frontiers*, 6(3): 357-372.
- Stampfli, G.M., Von Raumer, J. and Borel, G.D., 2002. Paleozoic evolution of pre-Variscan terranes: from Gondwana to the Variscan collision. In: J.R. Martínez Catalán, R.D. Hatcher, Jr., R. Arenas and F. Díaz García (Editors), *Variscan-Appalachian dynamics: the building of the Late Paleozoic basement*. Special publications. Geological Society of America, pp. 263-280.
- Stampfli, G.M., Hochard, C., Vérard, C., Wilhem, C. and Von Raumer, J., 2013. The formation of Pangea. *Tectonophysics*, 593: 1-19.
- Stern, C.R., 2011. Subduction erosion: rates, mechanisms, and its role in arc magmatism and the evolution of the continental crust and mantle. *Gondwana Research*, 20(2): 284-308.
- Stern, R.J., 2008. Modern-style plate tectonics began in Neoproterozoic Time: an alternative interpretation of earth's tectonic history. In: K. Condie and V. Pease (Editors), *When did Plate Tectonics Begin?*. Geological Society America Special Paper, pp. 265–280.

- Stevens, G., Clemens, J.D. and Droop, G.T.R., 1997. Melt production during granulite-facies anatexis: experimental data from "primitive" metasedimentary protoliths. *Contribution to Mineralogy and Petrology*, 128: 352-370.
- Stevens, G., Villaros, A. and Moyen, J.-F., 2007. Selective peritectic garnet entrainment as the origin of geochemical diversity in S-type granites. *Geology*, 35(1): 9-12.
- Streckeisen, A., 1976. To Each Plutonic Rock Its Proper Name. *Earth-Science Reviews*, 12(1): 1-33.
- Taylor, S.R. and McLennan, S.M., 1995. The geochemical evolution of the continental crust. *Reviews of Geophysics*, 33: 241-265.
- Turpin, L., Velde, D. and Pinte, G., 1988. Geochemical Comparison between Minettes and Kersantites from the Western European Hercynian Orogen - Trace-Element and Pb-Sr-Nd Isotope Constraints on Their Origin. *Earth and Planetary Science Letters*, 87(1-2): 73-86.
- Turpin, L., Cuney, M., Friedrich, M., Bouchez, J.L. and Aubertin, M., 1990. Meta-Igneous Origin of Hercynian Peraluminous Granites in Nw French Massif Central - Implications for Crustal History Reconstructions. *Contributions to Mineralogy and Petrology*, 104(2): 163-172.
- Ulmer, P., Muntener, O. and Perez, R.A., 2008. Differentiation of mantle-derived calc-alkaline magmas at mid to lower crustal levels: Experimental and petrologic constraints. *Geochimica et Cosmochimica Acta*, 72(12): A966-A966.
- Valley, J. et al., 2005. 4.4 billion years of crustal maturation: oxygen isotope ratios of magmatic zircon. *Contributions to Mineralogy and Petrology*, 150(6): 561-580.
- van Hunen, J. and Moyen, J.-F., 2012. Archaean subduction: fact or fiction? *Annual Review of Earth and Planetary Sciences*, 40: 195-219.
- Van Kranendonk, M.J., Hickman, A.H., Smithies, R.H. and Champion, D.C., 2007. Paleoproterozoic development of a continental nucleus: the East Pilbara terrane of the Pilbara craton, Western Australia. In: M.J. Van Kranendonk, R.H. Smithies and V. Bennet (Editors), *Earth's Oldest rocks. Developments in Precambrian Geology*. Elsevier, pp. 307-337.
- Vanderhaeghe O., (2004). Structural development of the Naxos migmatite dome. In: Gneiss Domes in Orogeny, Whitney D.L., Teyssier C., and Siddoway C.S. editors, *Geological Society of America Special Paper*, 380, 211-227.
- Vanderhaeghe, O., 2012. The thermal-mechanical evolution of crustal orogenic belts at convergent plate boundaries: a reappraisal of the orogenic cycle. *Journal of Geodynamics*, 56: 124-145.
- Vanderhaeghe, O. and Duchene, S., 2010. Crustal-scale mass transfer, geotherm and topography at convergent plate boundaries. *Terra Nova*, 22: 315-323.
- Vanderhaeghe, O. and Grabkowiak, A., 2014. Tectonic accretion and recycling of the continental lithosphere during the Alpine orogeny along the Pyrenees. *Bulletin de la Societe Geologique de France*, 185(4): 257-277.
- Vanderhaeghe, O., Gardien, V., Moyen, J.F., Laurent, O., Couzinié, S., Gébelin, A., Villaros, A., Ohnenstetter, D., 2014. Flow of the partially molten Variscan orogenic crust from syn-orogenic exhumation of subducted continental crust to gravitational collapse along a convergent plate boundary marked by slab retreat, 24e Réunion des Sciences de la Terre, Pau.
- Venables, W.N. and Ripley, B.D., 2002. *Modern Applied Statistics with S*. Springer.
- Villaros, A., Stevens, G. and Buick, I.S., 2009a. Tracking S-Type Granite from Source to Emplacement: Clues from Garnet in the Cape Granite Suite. *Lithos*, 112(3-4): 217-235.
- Villaros, A., Stevens, G., Moyen, J.-F. and Buick, I.S., 2009b. The trace element composition of S-type granites: evidence for disequilibrium melting and accessory phase entrainment in the source. *Contributions to Mineralogy and Petrology*, 158(4): 543-561.
- Villaros, A., Buick, I.S. and Stevens, G., 2011. Isotopic variations in S-type granites: an inheritance from a heterogeneous source? *Contribution to Mineralogy and Petrology*, 163(2): 243-257.
- Villaseca, C., Barbero, L. and Herreros, V., 1998. A re-examination of the typology of peraluminous granite types in intracontinental orogenic belts. *Transactions of the Royal Society of Edinburgh: Earth Sciences*, 89(02): 113-119.
- Watson, E. and Harrison, T., 1984. Accessory minerals and the geochemical evolution of crustal magmatic systems: a summary and prospectus of experimental approaches. *Physics of the Earth and Planetary Interiors*, 35(1): 19-30.

- Weber, C. and Barbey, P., 1986. The role of water, mixing processes and metamorphic fabric in the genesis of the Baume migmatites (Ardèche, France). *Contributions to Mineralogy and Petrology*, 92(4): 481-491.
- Wedepohl, K.H., 1995. The composition of the continental crust. *Geochimica et cosmochimica Acta*, 59(7): 1217-1232.
- Williamson, B., 1991. The petrology of the Velay granite complex. Massif Central, France. Ph. D. Thesis, Birkbeck College, London.
- Williamson, B.J., Downes, H. and Thirlwall, M.F., 1992. The Relationship between Crustal Magmatic Underplating and Granite Genesis - an Example from the Velay Granite Complex, Massif-Central, France. *Transactions of the Royal Society of Edinburgh-Earth Sciences*, 83: 235-245.
- Žák, J. et al., 2014. A plate-kinematic model for the assembly of the Bohemian Massif constrained by structural relationships around granitoid plutons. *Geological Society, London, Special Publications*, 405: SP405. 9.
- Zamora, D., 2000. Fusion de la croûte océanique subductée : approche expérimentale et géochimique. Thèse d'université Thesis, Université Blaise-Pascal, Clermont-Ferrand, France, 314 pp.
- Zeh, A., Brätz, H., L., M.I. and S., W.I., 2001. A combined zircon SHRIMP and Sm-Nd isotope study on high-grade paragneisses from the Mid-German Crystalline Rise: Evidence for northern Gondwanan and Grenvillian provenance. *Journal of the Geological Society of London*, 158: 983-994.
- Zeh, A. and Gerdes, A., 2010. Baltica- and Gondwana-derived sediments in the Mid-German Crystalline Rise (Central Europe): Implications for the closure of the Rheic ocean. *Gondwana Research*, 17: 254-263.
- Zeh, A., Stern, R.A. and Gerdes, A., 2014. The oldest zircons of Africa—Their U–Pb–Hf–O isotope and trace element systematics, and implications for Hadean to Archean crust–mantle evolution. *Precambrian Research*, 241: 203-230.

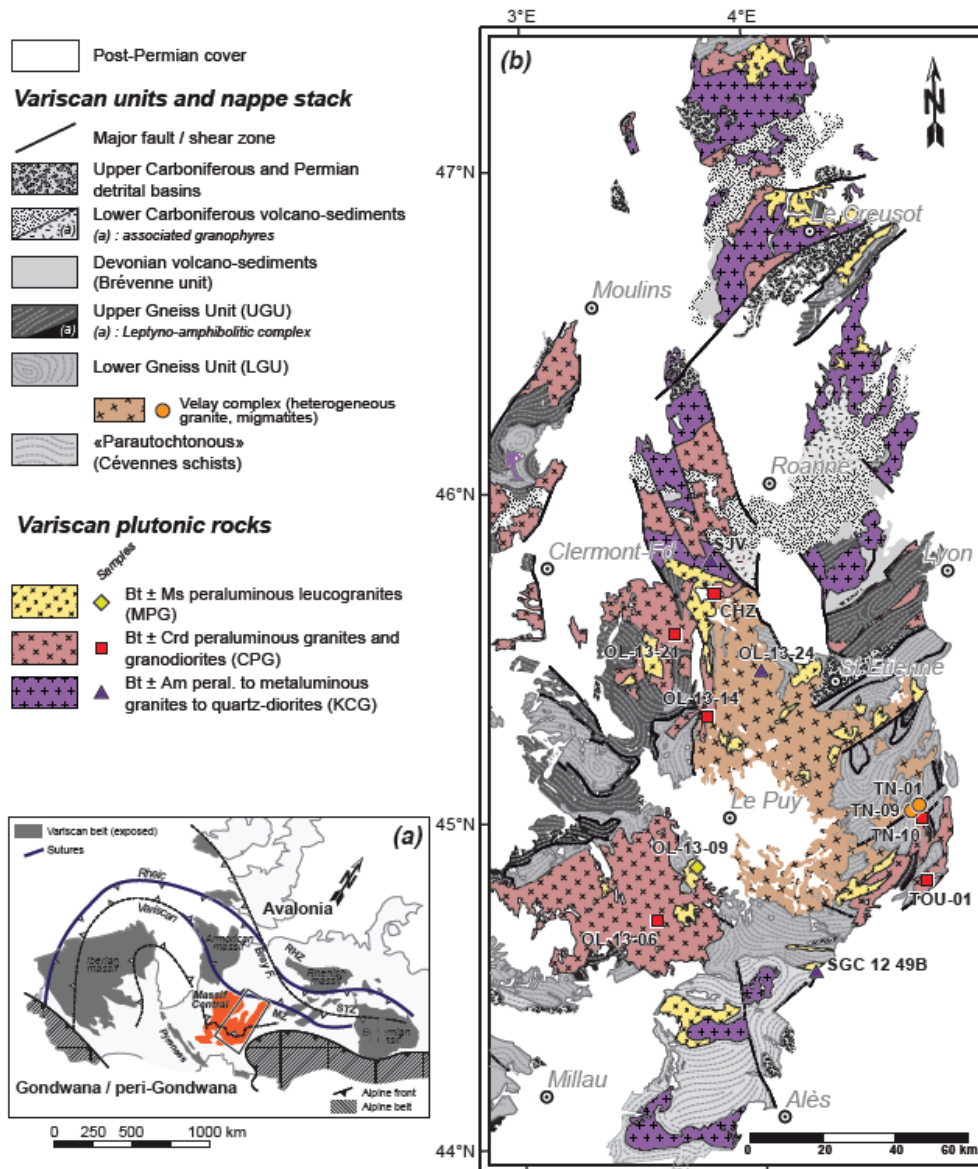


Figure 1

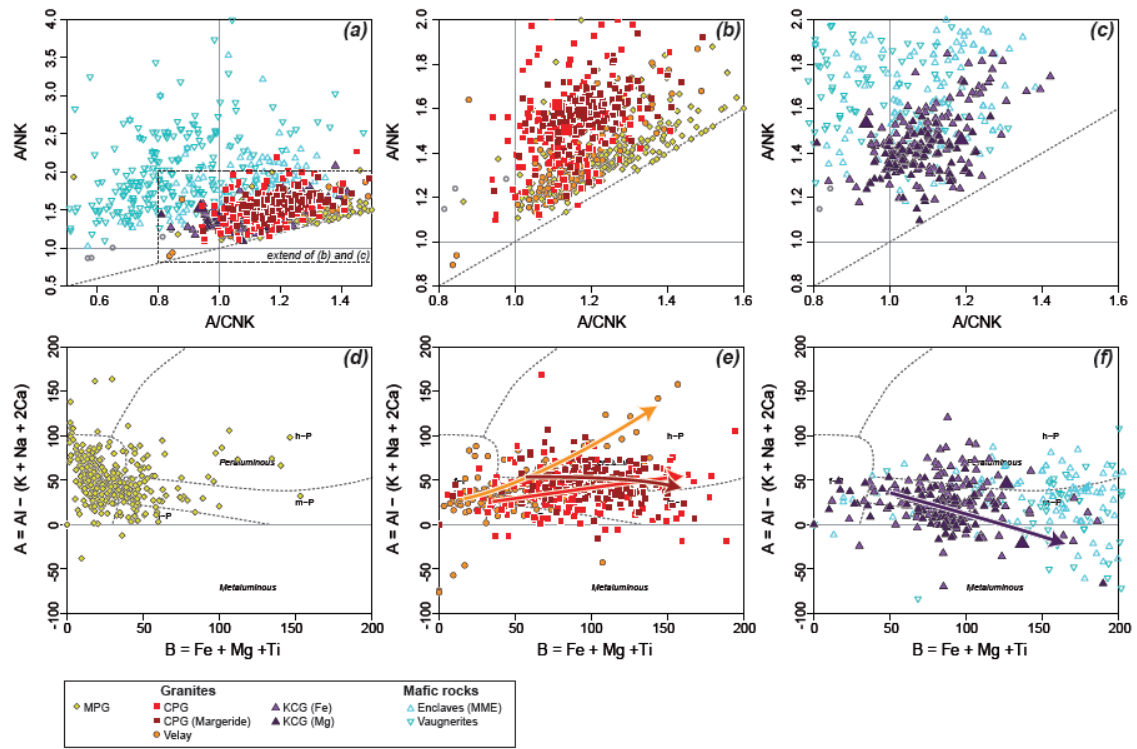


Figure 2

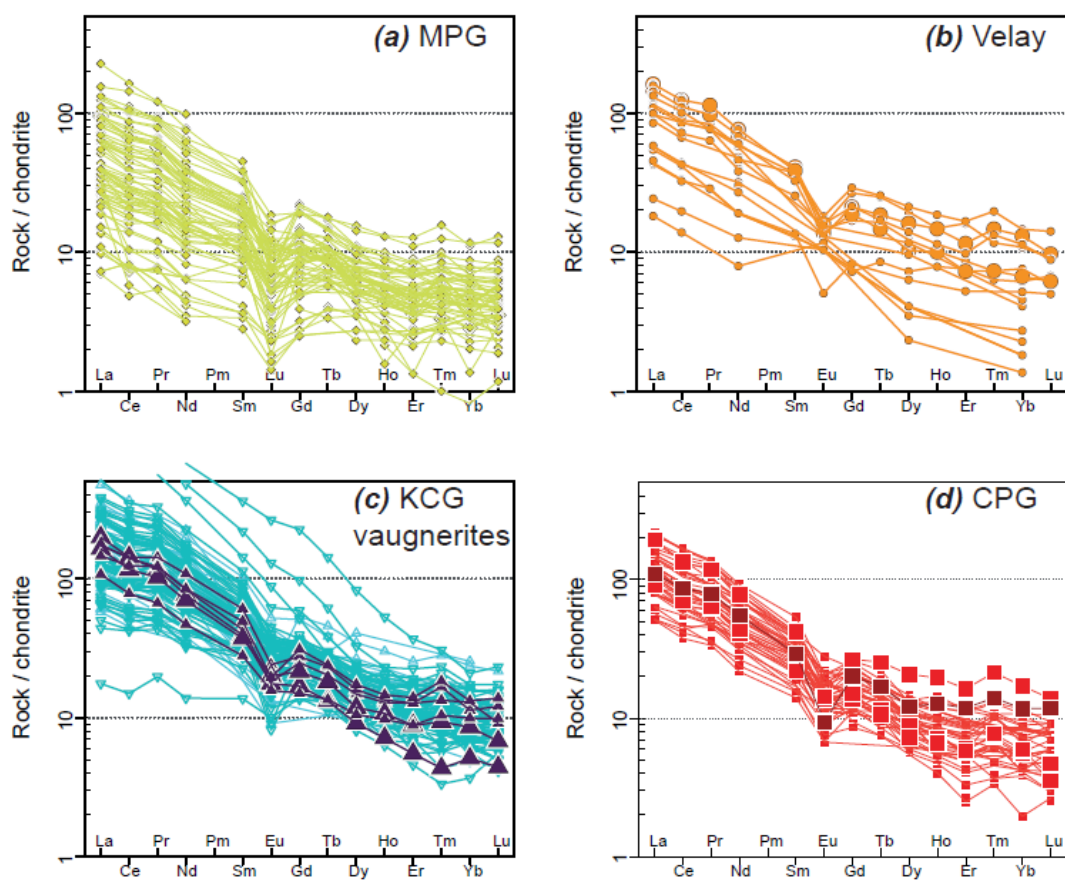


Figure 3



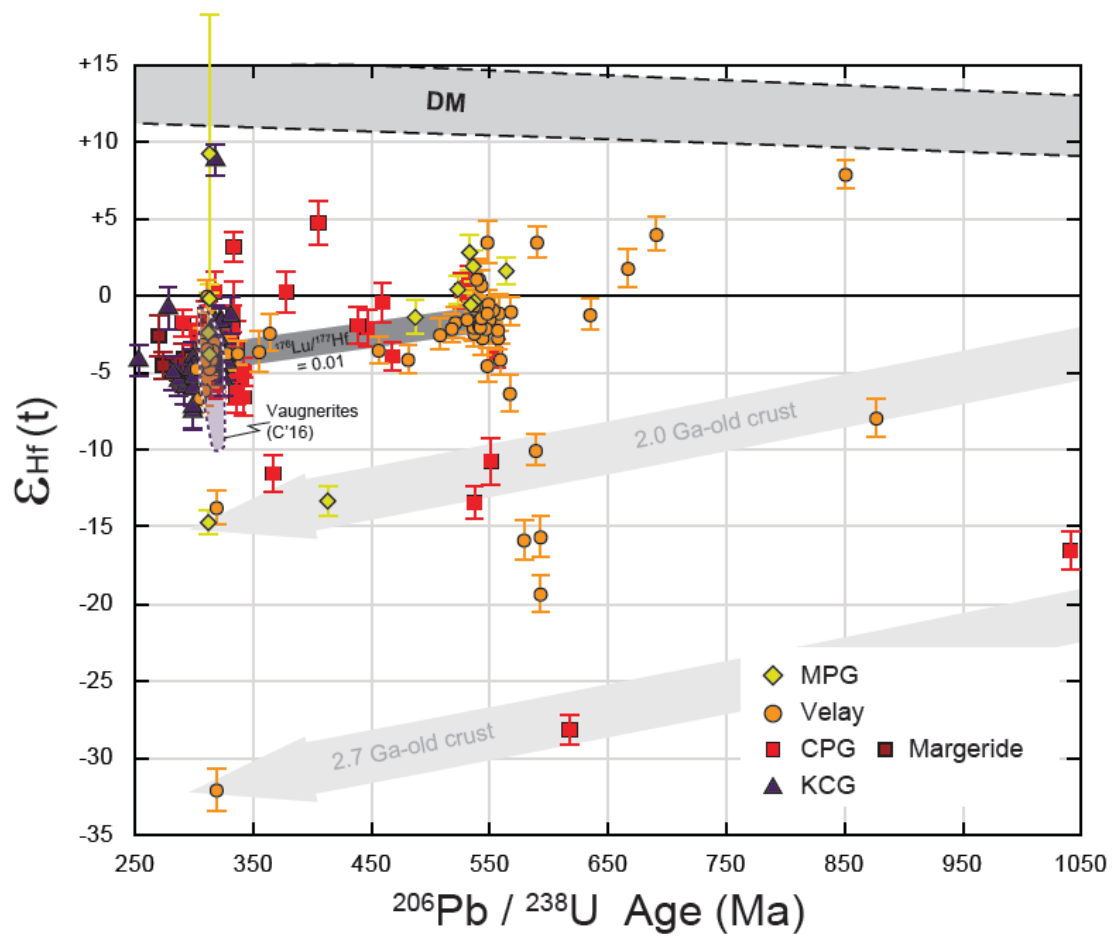


Figure 4

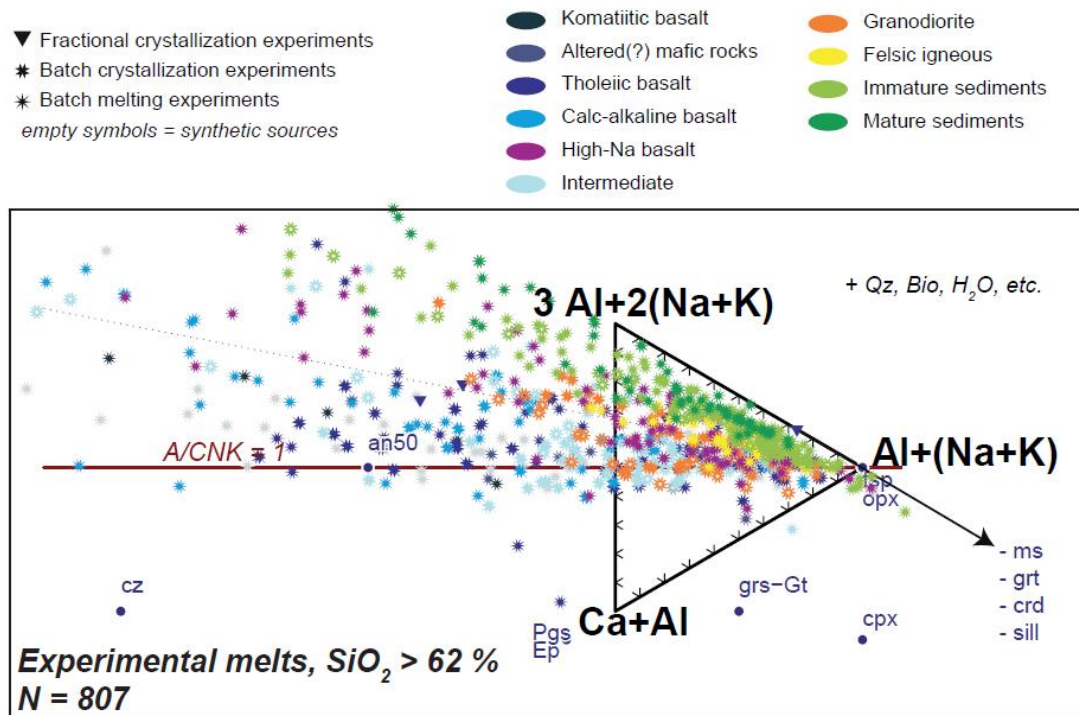


Figure 5

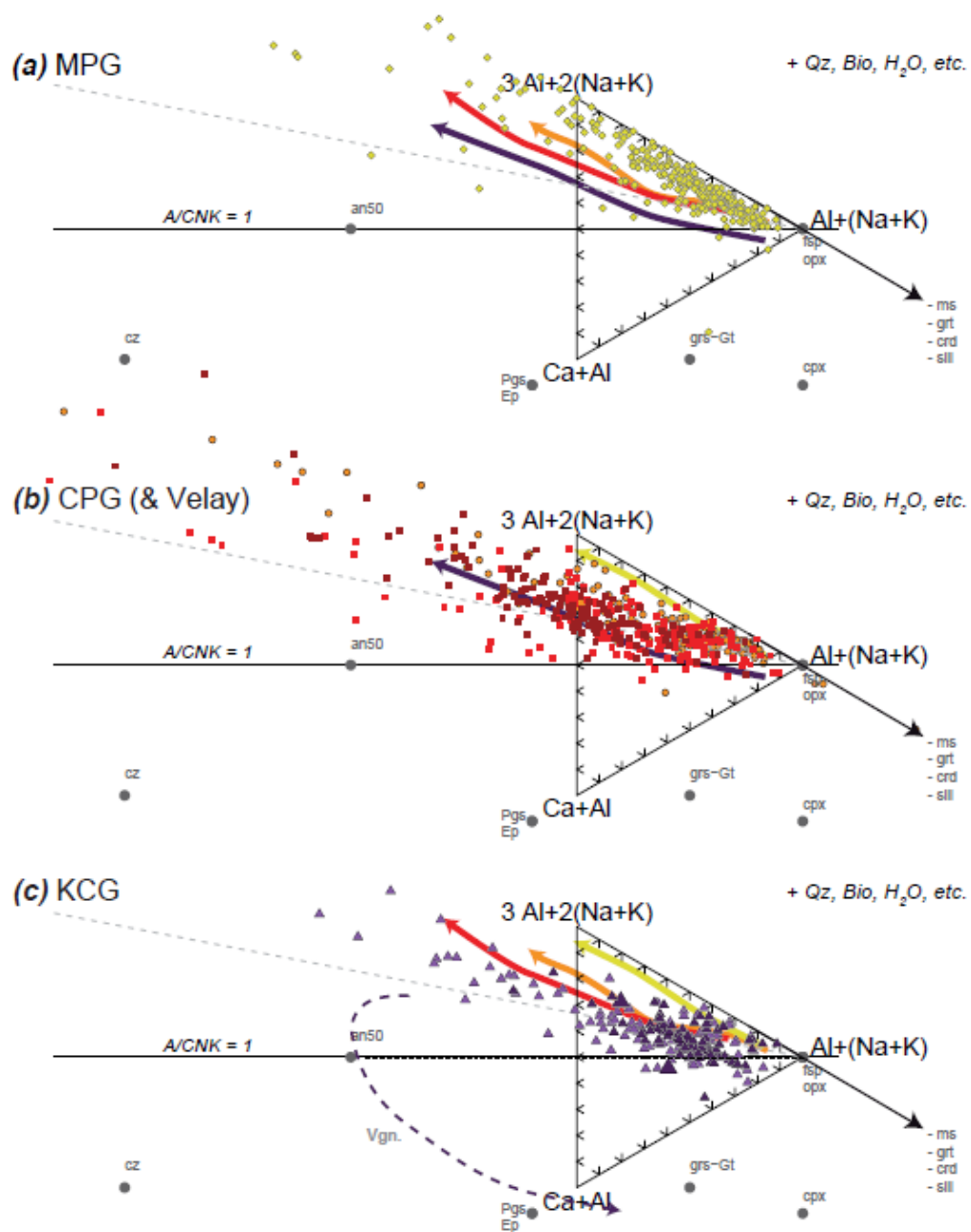


Figure 6

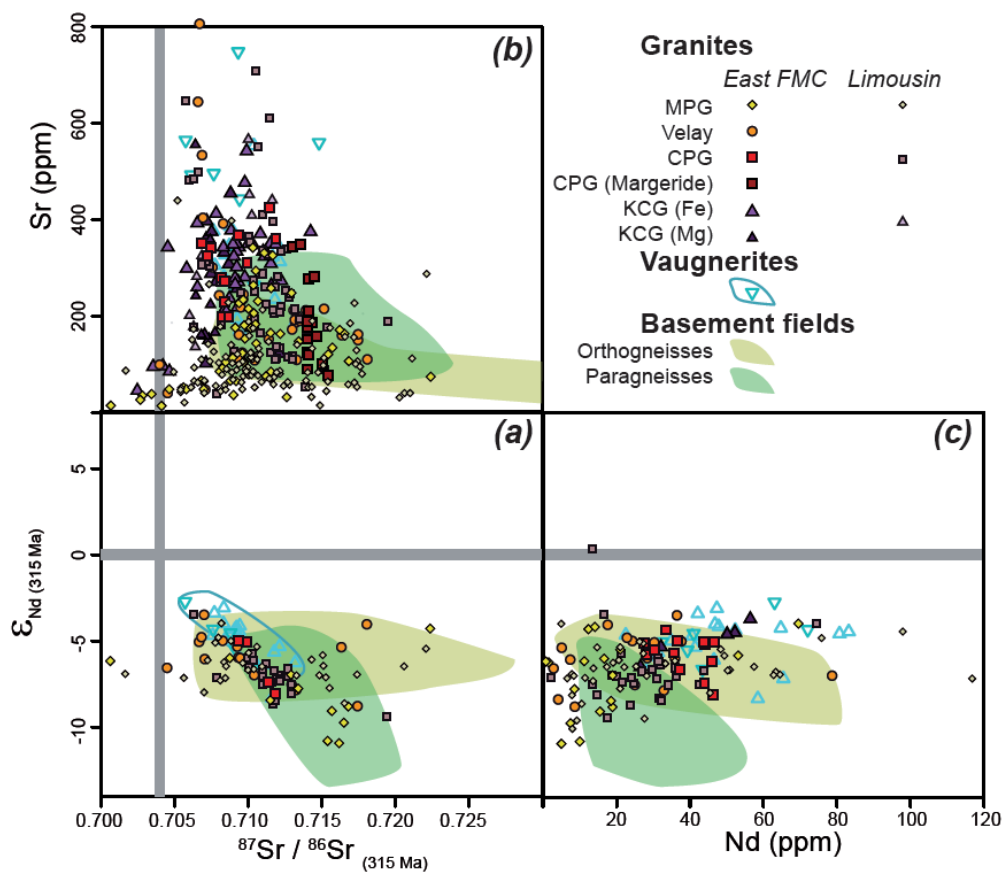


Figure 7

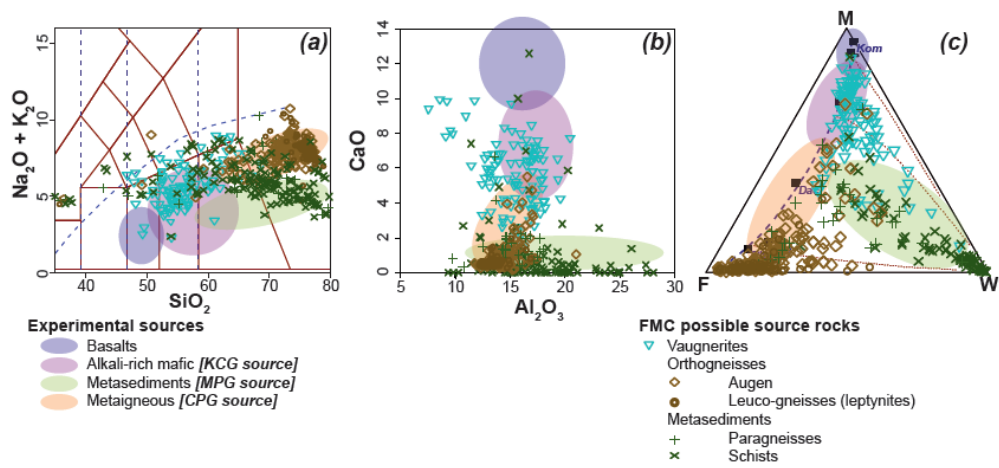


Figure 8

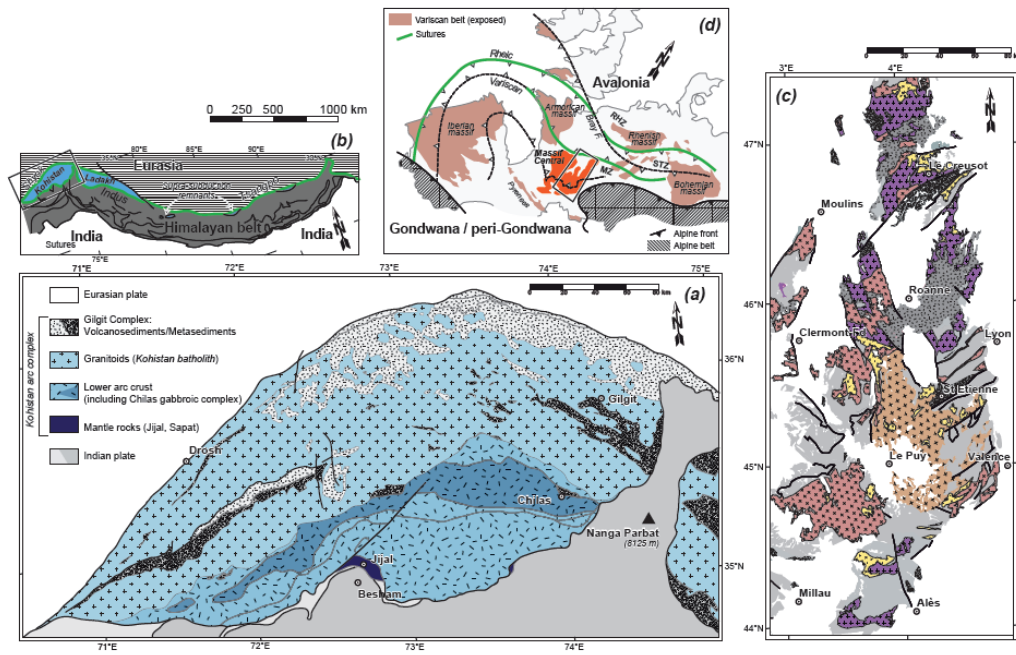


Figure 9

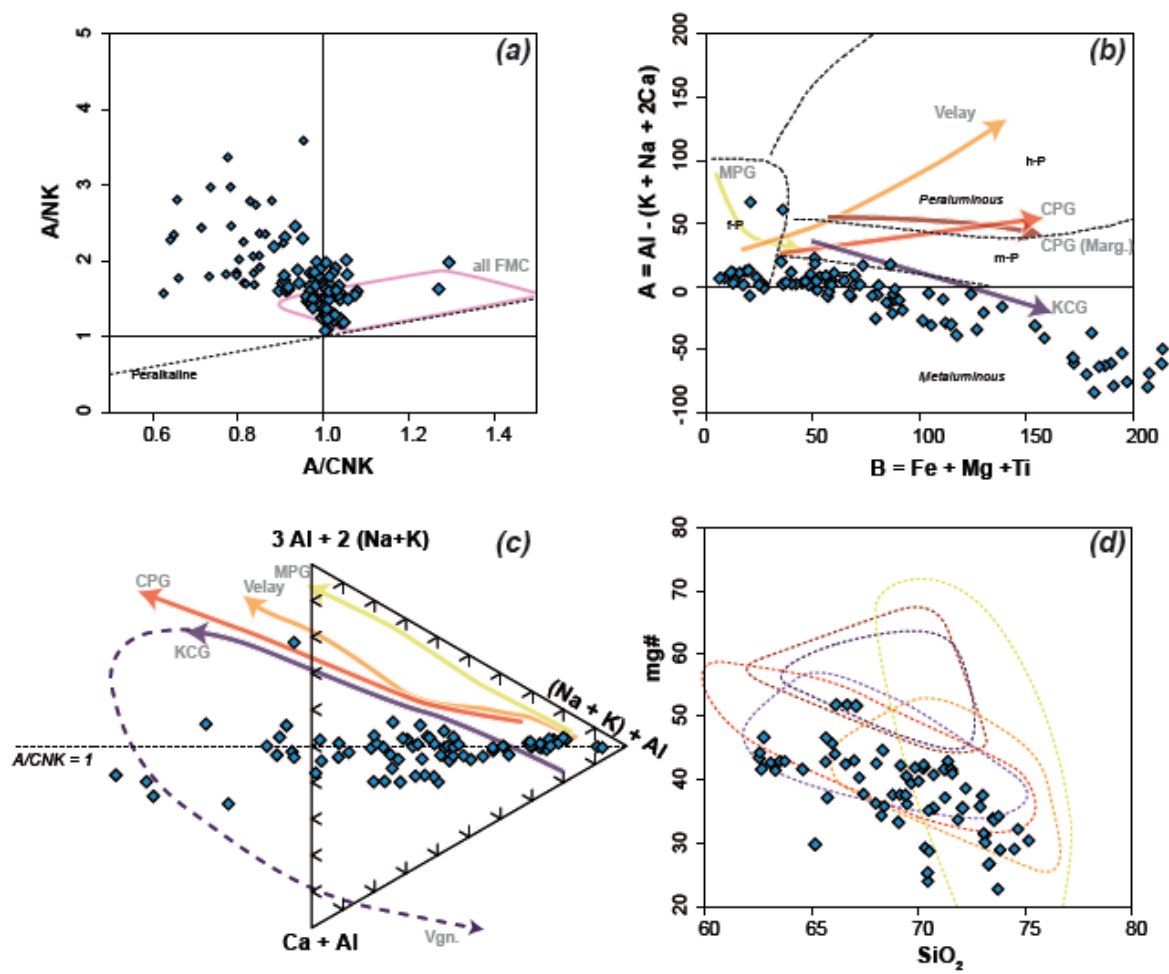


Figure 10

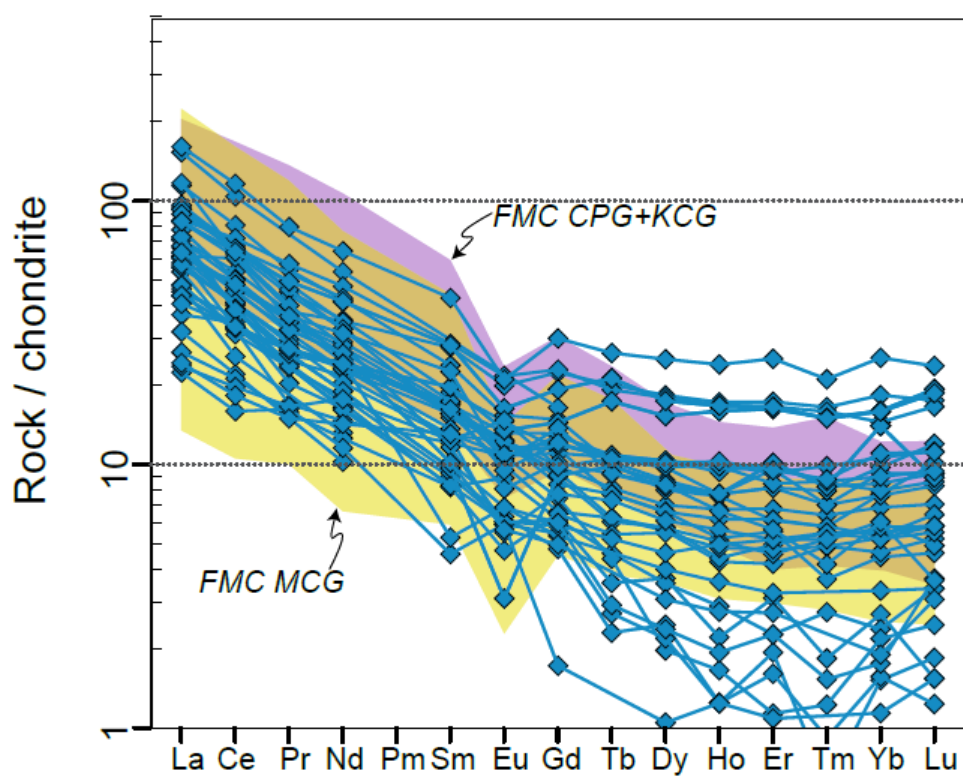


Figure 11



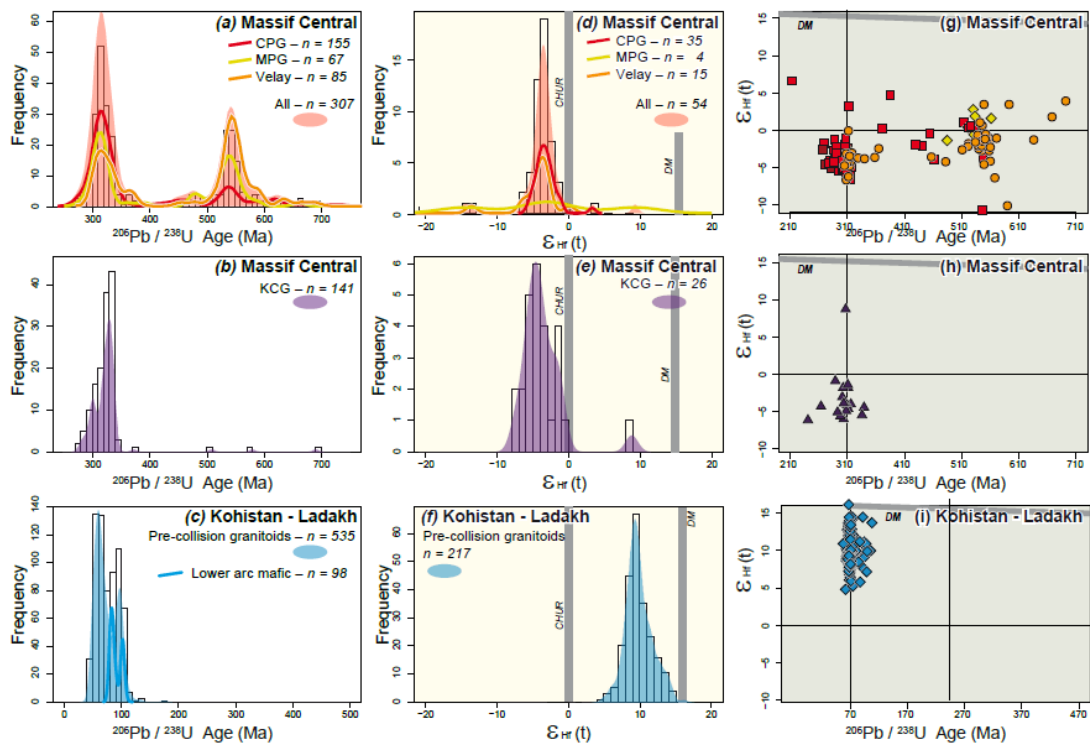


Figure 12

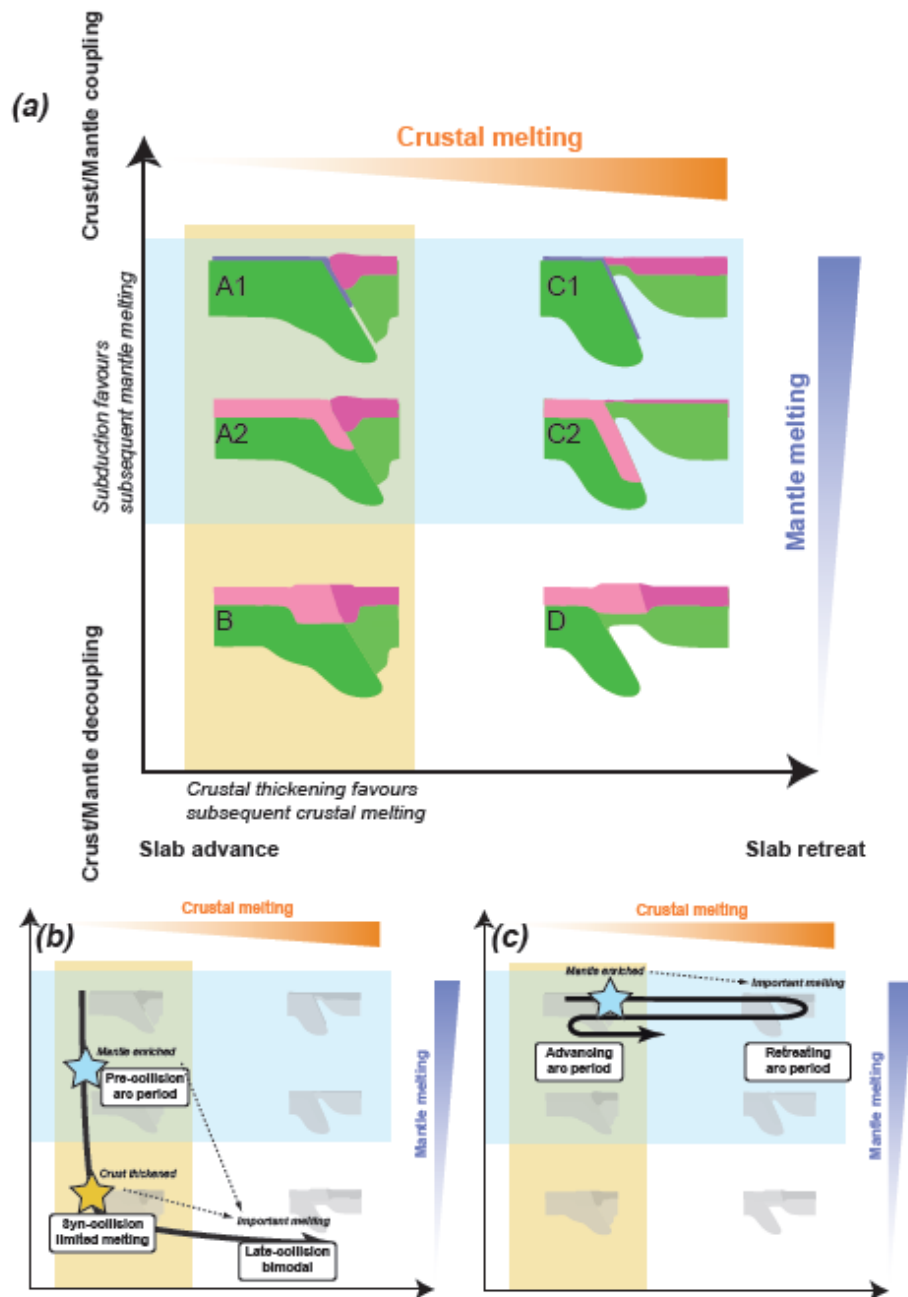


Figure 13

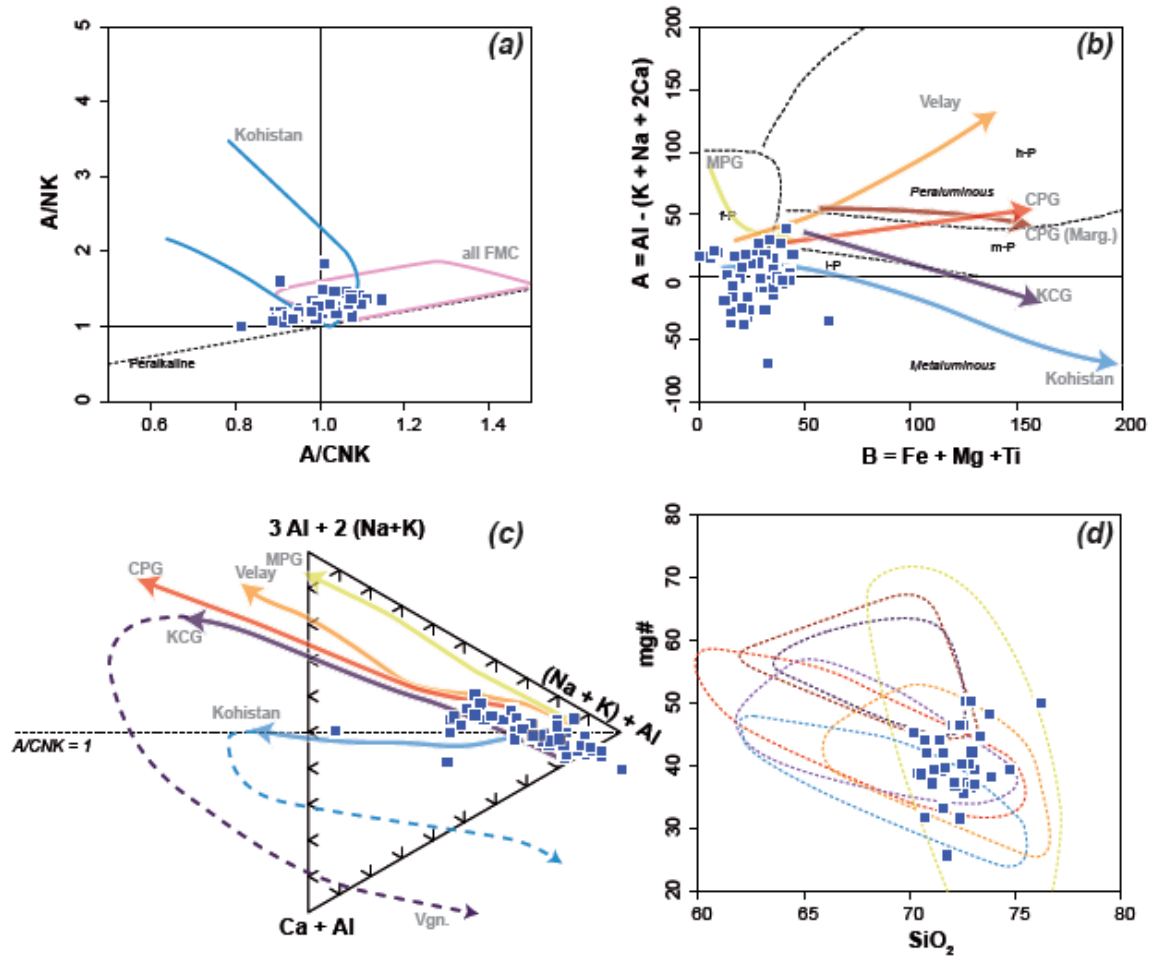


Figure 14

## Abstract

Earth's continental crust is dominantly made of buoyant, felsic igneous material (granitoids), that were ultimately extracted from the mantle as a result of Earth's differentiation. Since felsic melts are not in chemical equilibrium with the mantle, they can originate either from melting of older crustal lithologies, or from differentiation of a primitive mantle melt; only the latter case will contribute to crustal growth. To understand the mechanisms of continental crust growth and differentiation through time, it is therefore necessary to unravel the respective contribution of these two different mechanisms in the genesis of granitoid suites. In modern Earth, granitoids are chiefly generated in convergent plate boundaries (subduction and collision). This paper examines the granitic suites in a late-collision environment, the Variscan French Massif Central (FMC), and compares them with the suites found in an oceanic arc. We therefore describe, and compare, two end-members sites of granite generation.

In the FMC, several main types of granites are described. Muscovite and Cordierite bearing Peraluminous Granites (resp. MPG and CPG) contain large amounts of inherited zircons, and their chemistry demonstrates that their sources were older crustal material (resp. metasediments and metaigneous). On the other hand, Potassic Calc-alkaline Granites (KCG), associated to potassic diorites (vaugnerites) do not contain inherited zircons, and ultimately derive from the vaugnerites. The vaugnerites in turns form by partial melting of a mantle contaminated by the regional crust. Therefore, although they are isotopically similar to the crust, the KCG are net contributors to crustal growth. Thus we conclude that although late-orogenic settings are dominated by crustal melting and recycling, they may be sites of net crustal growth, even though this is not visible from isotopes only. In contrast, arc granitoids are purely or almost purely mantle derived. However, the preservation potential of arcs is much smaller than the preservation of late-orogenic domains, such that at the scale of a whole orogenic belt, late-orogenic magmatism is probably as important as arc magmatism.

Finally, we speculate that the situation may have been similar in the Archaean, or even more skewed towards late-orogenic sites (or similar environments, dominated by melting of a altered mafic protocrust), owing to the hotter mantle and less stable subductions during that period.

## Highlights :

- We describe the different granite types in a late collision environment, the Variscan French Massif Central (FMC).
- Besides abundant crustal melts, some granites are ultimately mantle-derived. However their isotopic properties are fully controlled by small amounts of crustal recycling to the mantle.
- This demonstrates that late-collision sites are a significant environment for crustal growth; although less efficient than supra-subduction arcs, they tend to be better preserved.
- We speculate that sites similar to late collision environments may be a realistic alternative to supra-subduction arcs for Archaean crustal growth.